Copyright

By

Craig Abel Rios

2007

Fatigue Performance of Multi-Sided High-Mast Lighting Towers

by

Craig Abel Rios, B.S.

Thesis

Presented to the Faculty of the Graduate School of
The University of Texas at Austin
in Partial Fulfillment
of the Requirements
for the Degree of

Master of Science in Engineering

The University of Texas at Austin
May 2007

Fatigue Performance of Multi-Sided High-Mast Lighting Towers

APPROVED BY
SUPERVISING COMMITTEE:

Supervisor: Karl H. Frank

Lance Manuel

Dedication

To my family.
Without your constant love, encouragement
and support this would not have been possible.

Acknowledgements

I would like to acknowledge the Texas Department of Transportation, the Pennsylvania Department of Transportation, the Iowa Department of Transportation, the Wyoming Department of Transportation, the Colorado Department of Transportation, the Minnesota Department of Transportation, the North Carolina Department of Transportation, the Wisconsin Department of Transportation, the California Department of Transportation, and the South Dakota Department of Transportation for funding this study of high-mast lighting towers and making my graduate education at the University of Texas possible.

To Dr. Frank, thank you for your guidance and mentoring throughout my graduate education. The knowledge I have learned from your anecdotes and life lessons is invaluable.

To Thomas Anderson, thanks for keeping the work day interesting. The hot summer days in the lab went much quicker with your humor and exuberance.

To Dennis Fillip, Blake Stasney, Greg Harris and the rest of the FSEL staff, thank you very much for your help during my project.

May 2007

Fatigue Performance of Multi-Sided High-Mast Lighting Towers

Craig Abel Rios, M.S.E
The University of Texas at Austin, 2007
SUPERVISOR: Karl H. Frank

This study investigated the fatigue performance of multi-sided high-mast lighting towers. Recent failures of high-mast lighting towers have increased the awareness of the problems associated with these cantilevered structures. The failures of these steel poles primarily occur just above the weld at the base plate connection indicating a fatigue type failure. Although these structures are designed to the current 2001 AASHTO Specification, their susceptibility to fatigue failure has become a nationwide problem.

The objective of this research was to evaluate the fatigue performance of typical fatigue critical connection details used in high-mast lighting towers. Laboratory fatigue testing was performed on full-scale specimens utilizing fillet welded socket connections, full penetration weld connections, as well as a stool base connection detail. The results of the study found that that the design provisions for high-mast lighting towers do not accurately predict the fatigue life of the structures. Common details designed in accordance with the AASHTO specification did not meet the required minimum fatigue life categories as specified by the design provisions. It was also found that significant fatigue resistance can be gained with an increase in base plate thickness and an increase in number of bolts used in the base plates.

Table of Contents

CHAPTER 1 INTRODUCTION 1

1.1 Background 1
1.2 High Mast Lighting Tower Features 3
1.3 Wind Loading 8
1.3.1 Natural Wind Gusts 8
1.3.2 Vortex Shedding 10
1.4 High Mast Lighting Tower Failures 11
1.5 High Mast Lighting Tower Design Using AASHTO 14
1.6 Related Research 15
1.6.1 Physical Testing 15
1.6.2 Analytical Modeling 16
1.7 Scope 17

CHAPTER 2 TEST SPECIMEN DESIGN 18

2.1 Specimen Design 18
2.2 Fillet Welded Socket Connection 19
2.3 Full Penetration Welded Connections 21
2.1.2 Wyoming Detail 21
2.1.3 Texas Detail 23
2.4 Stool Base Detail 24
2.4.1 Stool Base Stiffener Design 26
2.5 Test Matrix 28
2.6 Specimen Labels 29

CHAPTER 3 TEST SETUP 31

3.1 Design Decisions 31
3.2 Test Setup Design 33
3.2.1 Test Setup Length 33
3.2.2 Design of Loading Box 36
3.2.3 Dynamic Analysis of Test Setup 38
3.2.4 Design of Reaction Supports 39
3.2.5 Portal Loading Frame 41
3.3 MTS closed loop system 42

CHAPTER 4 TESTING PROCEDURE 45

4.1 General Test Procedure 45
4.1.1 Specimen Measurements 45
4.1.2 Specimen Installation Procedure 46
4.1.3 Calculation of Loads 49
4.1.4 Setting Deflections under Displacement Control 52
4.2 Testing Speed 52
4.3 Definition of Failure 52

CHAPTER 5 TEST RESULTS 53

5.1 Fatigue Test Results 53
5.1.1 Results for Fillet Welded Socket Connections 53
5.1.2 Results for Full Penetration Weld Connections 56
5.1.3 Results for Stool Base Detail Connections 60
5.1.4 General comparison of fatigue life for all connection types 62
5.2 Results of Tensile Tests and Chemistry Analysis 63
5.2.1 Tensile Test Results 63
5.2.2 Chemistry Analysis Results 64

CHAPTER 6 CONCLUSIONS AND RECOMMENDED RESEARCH 66

6.1 Conclusions 66
6.2 Recommended Research 67

APPENDIX A MEASURED DIMENSIONS OF TEST SPECIMENS 69

APPENDIX B CALCULATED LOADS AND DISPLACEMENTS FOR FATGIUE TESTING 76

REFERENCES 78

VITA 80

List of Tables

Table 2.1: Test matrix for 24-in high mast poles 29
Table 3.1: Stress and deflections from SAP 35
Table 3.2: Required Flow Calculations 35
Table 4.1: Verification of ultrasonic thickness measurements 45
Table 5.1: Fatigue testing results for fillet welded socket connection specimens 56
Table 5.2: Fatigue testing results for full penetration weld connection specimens60
Table 5.3: Fatigue testing results for stool base connection detail specimens..... 61
Table 5.4: Tensile test results..... 64
Table 5.5: Results of Chemistry Analysis..... 65
Table A1: General Dimensions- Diameters at base to flats 69
Table A2: General Dimensions- Diameter at base to corners..... 70
Table A3: General Dimensions- Diameter 12-in away from base to flats..... 70
Table A4: General Dimensions- Diameter 12-in away from base to corners..... 71
Table A5: General Dimensions- Base plate thickness 71
Table A6: General Dimensions- Pole wall thickness 72
Table A7: Socket Weld Dimensions- Long leg dimensions 72
Table A8: Socket Weld Dimensions- Short leg dimensions..... 73
Table A9: Full Penetration Weld Dimensions- Long leg dimensions 73
Table A10: Full Penetration Weld Dimensions- Short leg dimensions 73
Table A11: Stool Base Detail Dimensions- Stiffener dimensions..... 74
Table B1: Calculate properties from AutoCAD using average dimensions 76
Table B2: Calculated ram loads to achieve desired stresses..... 76
Table B3: Testing displacements and corresponding values 77

List of Figures

Figure 1.1 High-mast lighting towers at a highway intersection 2
Figure 1.2: Typical high-mast lighting tower 3
Figure 1.3: High-mast lighting tower foundation 4
Figure 1.4: Typical high-mast tower base plate to foundation connection 5
Figure 1.5: Example of socketed connection (Courtesy of Valmont Industries) 6
Figure 1.6: Example of full penetration weld connection (Courtesy of Valmont Industries) 6
Figure 1.7: High-mast pole sections and lighting apparatus 7
Figure 1.8: Hand access hole for winch system 8
Figure 1.9: von Karman Vortex Street (courtesy of Google Images) 10
Figure 1.10: Failure of high mast lighting tower in Rapid City, South Dakota (Courtesy of Rapid City Journal) 12
Figure 1.11: Remaining intact base plate in South Dakota (Courtesy of Rapid City Journal) 13
Figure 1.12: Failure in Colorado 14
Figure 2.1: Test specimen fabrication drawing 19
Figure 2.2: Fillet welded socket connection detail 20
Figure 2.3: Socket connection weld detail 20
Figure 2.4: Wyoming connection detail 22
Figure 2.5: Wyoming connection weld detail 22
Figure 2.6: Texas connection detail 23
Figure 2.7: Texas connection weld detail 24
Figure 2.8: U-Rib stiffened horizontal mast-arm 24
Figure 2.9: Stool base connection detail 25
Figure 2.10: Stool chair detail 25
Figure 2.11: Base plate weld detail for stool base connection 26
Figure 2.12: Free-body diagram for vertical stiffener plates 27

Figure 2.13: Labeling system used for high-mast specimens 30
Figure 3.1: Vertical test setup option 31
Figure 3.2: Tension test setup 32
Figure 3.3: Illustration of SAP model 34
Figure 3.4: Fabrication drawing of loading box 36
Figure 3.5: Leveling nuts used for base plate to loading box connection 37
Figure 3.6: Single degree of freedom system used for dynamic analysis 38
Figure 3.7: 1 Degree of freedom reaction support 40
Figure 3.8: 2 degree of freedom reaction support 41
Figure 3.9: Portal loading frame showing lateral bracing 42
Figure 3.10: Error during low frequency cyclic testing 43
Figure 3.11: Error during high frequency cyclic testing 43
Figure 4.1: Pole specimens released from reaction supports 47
Figure 4.2: Transfer of reaction plates to new specimens 48
Figure 4.3: Moment diagram for calculation of stresses 49
Figure 4.4: Spreadsheet used for calculation of testing loads 51
Figure 5.1: Typical failure of fillet welded socket connection 54
Figure 5.2: Etched cross section of fillet welded socket connection 55
Figure 5.3: Typical failure of Wyoming full penetration weld connection 57
Figure 5.4: Typical Failure of Texas full penetration weld connection 57
Figure 5.5: Etched cross section of Wyoming full penetration weld connection 58
Figure 5.6: Etched cross section of Texas full penetration weld connection 59
Figure 5.7: Typical failure of stool base detail connection 61
Figure 5.8: S-N plot of fatigue test results for all connection types 62
Figure 5.9: Tensile test results for pole wall steel coupons 63
Figure A1: Locations of dimensions for stool base stiffeners 75

CHAPTER 1

Introduction

1.1 BACKGROUND

This study investigated the fatigue performance of multi-sided high-mast lighting towers. Recent failures of high-mast lighting towers have increased the awareness of the problems associated with these cantilevered structures. The failures of these steel poles primarily occur just above the weld at the base plate connection indicating a fatigue type failure. Although these structures are designed to the current 2001 AASHTO Specification, their susceptibility to fatigue failure has become a nationwide problem.

High-mast lighting towers are vertical, cantilevered structures that are used to illuminate a relatively large area. Although primarily used for highway intersection lighting in rural areas, they are also utilized in other large areas such as parking lots, sporting venues, or even penitentiaries. As a result, failures of these structures are critical due to the potential for them to fall across highway lanes or other occupied areas.

High-mast lighting dates back to the 1800's when tall masts were installed in several cities to illuminate large areas. The first known application of high-mast lighting to highways was the Heerdter Triangle installation in Dusseldorf, Germany, in the late 1950's. It was followed by installations in other European countries including Holland, France, Italy, and Great Britain. With the passing of the Federal Aid Highway Act of 1956, interest in high-mast lighting in this country was stimulated by the successful applications in Europe (Walton, 1969).

In the late 1960's, studies were conducted to investigate the impact that high-mast lighting has on driver visibility, traffic performance, and illumination costs. It was found that increasing the height of the lighting offered a noticeable advantage in that it provided drivers with increased uniformity of illumination and brightness while minimizing

discomfort and disability glare. This, in turn, led to a reduced number of visibility related accidents (Walter, 1967).

Figure 1.1 High-mast lighting towers at a highway intersection

Figure 1.1 shows a highway intersection located in northwest Austin, Texas. At this intersection there are twenty-three high mast lighting towers used to illuminate the highways. Each contributes to the probability of failure in fatigue of a tower at this intersection. Although the towers increase illumination while keeping glare at a minimum, their location next to highly occupied areas in conjunction with their susceptibility to failure in fatigue could lead to a dangerous event.

1.2 HIGH MAST LIGHTING TOWER FEATURES

High-mast lighting towers have several distinct features. The towers consist of a single sectioned tube connected to a flat base plate. Base plates range from 1.5-in to 4-in in thickness. The base plate is bolted to a concrete foundation that extends several feet into the ground. Illumination comes from a lighting apparatus located at the top of the tower. Figure 1.2 shows a typical high-mast lighting tower.

Figure 1.2: Typical high-mast lighting tower

The concrete foundation, as shown in Figure 1.3, extends several feet into the ground. The foundation may extend up to forty feet into the ground, depending on local geological conditions. Drilled shafts are typically used for foundations; however, piles or spread footings may also be used if local conditions warrant.

Figure 1.3: High-mast lighting tower foundation

Anchor rods are used to connect the high-mast base plate to the concrete foundation. The size and number of anchor rods used are determined by the size and height of the high-mast tower. The anchor rods extend into the concrete foundation a considerable depth to prevent anchorage failure.

Nuts are used on both the top and bottom of the tower base plate. Leveling nuts are used underneath the base plate to both level the tower during erection and provide uniform tightening of the base plate. The top nuts tighten the base plate to the leveling nuts which fixes the entire system to the concrete foundation. It is important to note that improper tightening of the nuts can introduce additional stresses in the pole to base plate connections. This is believed to be the culprit of many high-mast tower failures. In order

to prevent loosening of the top nuts, double nuts are commonly used on the top side of the base plate. As an alternative, a tack weld can also be used as shown in Figure 1.4.

Figure 1.4: Typical high-mast tower base plate to foundation connection

The pole wall of the high-mast towers is typically connected to the base plates by either using a socketed connection or a full penetration weld connection. In the socketed connection, a hole is cut into the base plate that is the same diameter as the pole. The pole is then inserted into the base plate "socket," and a structural weld is run on the exterior of the pole wall connecting the pole to the base plate. An additional weld is run on the inside of the socket to provide additional strength as well as prevent corrosion in the gap between the pole wall and the base plate. In the full penetration weld connection, the pole is butted up against the base plate. A bevel is cut into the pole wall that allows full penetration of the structural weld on the outside of the pole wall. A small fillet weld

is then run on the inside of the pole wall to eliminate initial crack defects and to prevent corrosion. Figures 1.5 and 1.6 show examples of socketed connections and full penetration weld connections, respectively.

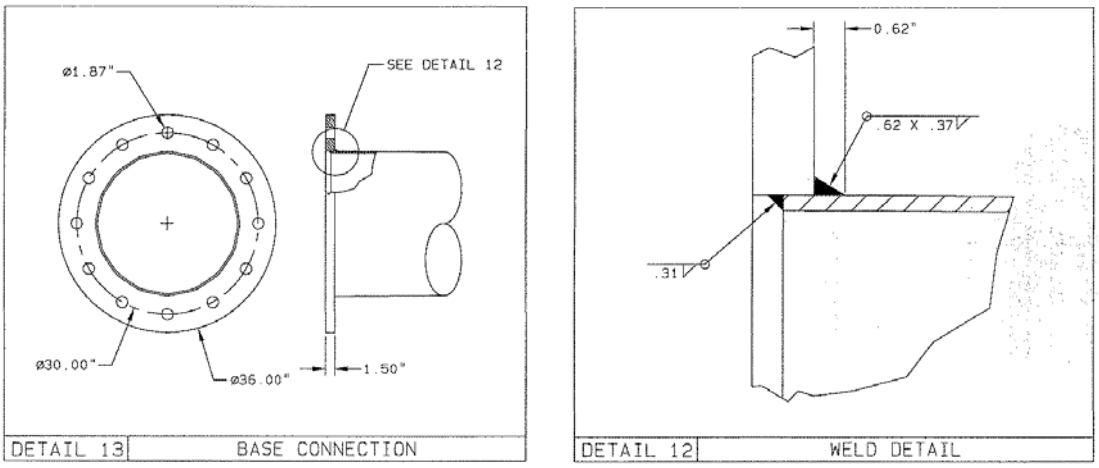

Figure 1.5: Example of socketed connection (Courtesy of Valmont Industries)

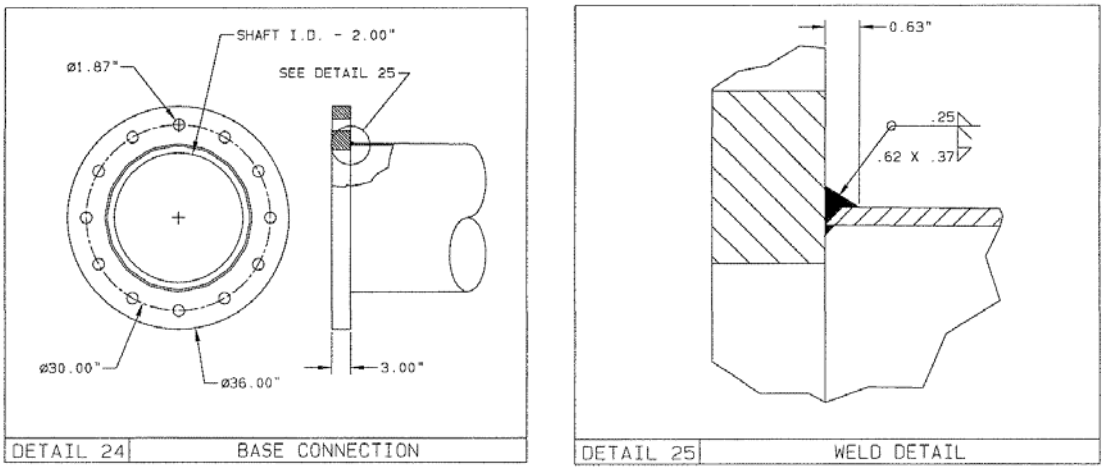

Figure 1.6: Example of full penetration weld connection (Courtesy of Valmont Industries)

Due to the large diameter of the poles used in high-mast lighting towers, the steel plate used in fabrication is not able to be formed into a round section in a practical

manner. Instead, the steel plate is formed into a polygonal shape using a break press. This approximates the round section desired. The number of polygonal sides used in the forming of the section depends on the size and diameter of the tower.

Due to the height of high mast lighting towers, the poles are sectioned into lengths of approximately fifty feet. At the point of the section splice, the upper section is fabricated so that it fits around the lower section. Figure 1.7 shows a high-mast tower that is composed of three pole sections with two splices.

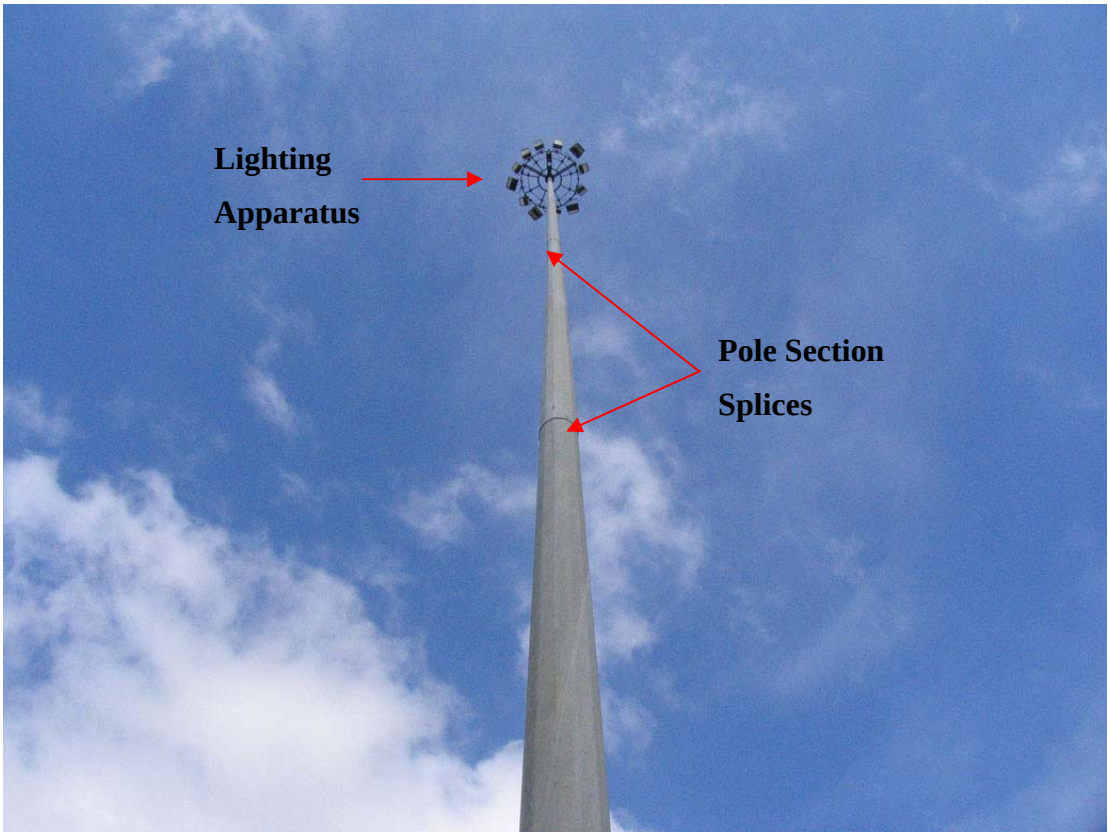

Figure 1.7: High-mast pole sections and lighting apparatus

The lighting apparatus located at the top of the high-mast lighting tower is held in place by a winch system that runs the entire height of the structure. The winch system allows the light apparatus to be raised and lowered for maintenance. Figure 1.8 shows the access hole that allows the winch system to be controlled from ground level.

Figure 1.8: Hand access hole for winch system

1.3 WIND LOADING

On high-mast lighting towers, there exists both dead and live load. The dead load is present due to the weight of the lighting apparatus. The live load on the structure is wind induced. There are two types of wind induced loads on the towers. The first is the loading due to natural wind gusts; the second is due to vortex shedding.

1.3.1 Natural Wind Gusts

Wind, or the motion of air with respect to the earth, is caused by variable solar heating in the earth's atmosphere. It is due to the difference in pressures in areas that have differing temperatures. Natural wind gusts occur due to the fluctuations in the flow of wind. For structures with very low damping, the structural response to natural wind gusts is determined by the natural frequency of the structure. Since wind gusts are highly

variable in velocity and direction, accumulation of fatigue loading cycles from wind gusts is less of a concern than those from a constant-amplitude harmonic response such as that due to vortex shedding (Simiu, 1996).

In the AASHTO design code, normal wind pressures are addressed in relation to ultimate strength design. The design wind pressure as presented in the code is a function of height and exposure of the structure, a wind gust factor, a 3-sec gust velocity, and the drag coefficient of the cross section of the structure. The wind pressure equation used by the AASHTO design code can be seen in Equation 1.

$$P_Z = 0.00256 \cdot K_Z \cdot G \cdot V^2 \cdot I_r \cdot C_d \text{ (psf)} \qquad (1)$$

K_Z represents the height and exposure factor. The height and exposure factor varies with height above the ground depending on local exposure conditions. G represents the wind gust factor which corrects the effective velocity pressure for the dynamic interaction of the structure with the gustiness of the wind. V is the 3-sec gust velocity which varies by location. I_r represents the wind importance factor that allows the wind pressures associated with the 50-year mean recurrence interval (3-sec gust wind speeds) to be adjusted to represent wind pressures associated with 10, 25, or 100 year mean recurrence intervals. This was incorporated into the equation due to the significant difference in design pressures of non-hurricane and hurricane winds. C_d is the wind drag coefficient which is associated with the cross section of the structure (AASHTO, 2001).

With respect to fatigue design, high-level lighting supports are designed to resist an equivalent static natural wind gust pressure range given by Equation 2. In Equation 2, C_d represents the drag coefficient of the cross section of the structure and I_f represents the fatigue importance factor. The fatigue importance factor accounts for the degree of hazard to traffic and damage to property that might occur should the structure fail. Importance factors range from a value of 1 for critical structures installed next to major highways to 0.44 for structures not installed next to major or secondary highways. The fatigue importance factor is determined by the owner of the structure.

$$P_{NW} = 5.2 C_d I_f \text{ (psf)} \qquad (2)$$

Once the stress range is known, details on the structure must meet stress categories stipulated by the AASHTO design code. In the case of high-mast lighting towers, the pole to base plate connection is classified as a category E detail if using a full-penetration groove-weld or a category E' for a fillet welded socket connection. A category E' detail represents a constant amplitude fatigue life (CAFL) threshold of 2.6 ksi whereas a category E detail represents a CAFL threshold of 4.5 ksi.

1.3.2 Vortex Shedding

Vortex shedding is a natural wind phenomenon that typically develops during steady, uniform wind flow and produces resonant oscillations in a plane normal to the direction of flow. For slender cylindrical structures, vortices, such as those seen in Figure 1.9, are shed along the direction of the wind alternatively to the left and right of the cross section in a pattern called a von Karman vortex street. This produces pulsating excitation forces in the direction perpendicular to the wind flow. If vortices are shed at the same period as the structure; the structure can be significantly excited especially in the bending mode (Sockel, 1994).

Figure 1.9: von Karman Vortex Street (courtesy of Google Images)

If the vortex frequency, f_v, is the same as the natural bending frequency, f_n, of the structure resonance occurs at the critical wind speed, V_{cr}, which can be found in Equation 3 for a cylindrical cross section (Sockel, 1994).

$$V_c = \frac{f_n D}{S} \qquad (3)$$

In the critical wind speed equation, f_n represents the natural frequency of the structure, D is the diameter of the cylinder, and S is the Strouhal number. In the AASHTO design specification, lighting structures are design to resist vortex shedding-induced loads for critical wind velocities less than 45 mph. The code uses the critical wind velocity from Equation 2 to find an equivalent static pressure range to be used for the design of vortex shedding-induced loads. The equation for the equivalent static pressure range can be found in Equation 4.

$$P_{VS} = \frac{0.00118 \cdot V_c^2 C_d I_F}{2\beta} \text{ (psf)} \qquad (4)$$

In Equation 4, V_c, C_d, and I_F are the same as previously defined. The term β represents the damping ratio of the structure. The AASHTO code allows β to be conservatively taken as .005. Once the equivalent static stress range is known, details on the structure must meet the previously mentioned stress categories stipulated by the AASHTO design code. It should be noted that the distribution of forces varies along the height of the structure since high-mast lighting towers are designed with a tapered pole shaft.

1.4 HIGH MAST LIGHTING TOWER FAILURES

Several failures of high mast lighting towers have occurred across the country. Although these failures have not resulted in any known fatalities, they have grown concern in the fatigue performance of these cantilevered structures.

Two such failures occurred at the same highway intersection near Rapid City, South Dakota. The first failure occurred in December of 2005 when a tower fell onto the westbound off-ramp of Highway 90. The second failure occurred four months later in April of 2006 when another tower fell onto a westbound on-ramp during a snowstorm.

These failures are examples of the danger associated with the failures of these structures due to their close proximities to occupied areas. Figure 1.10 shows the close proximity of the towers to the adjacent highway. As a result of the two failures, eleven towers around Rapid City with similar designs were taken down as a precaution. A state wide inspection of about 136 towers was also instituted.

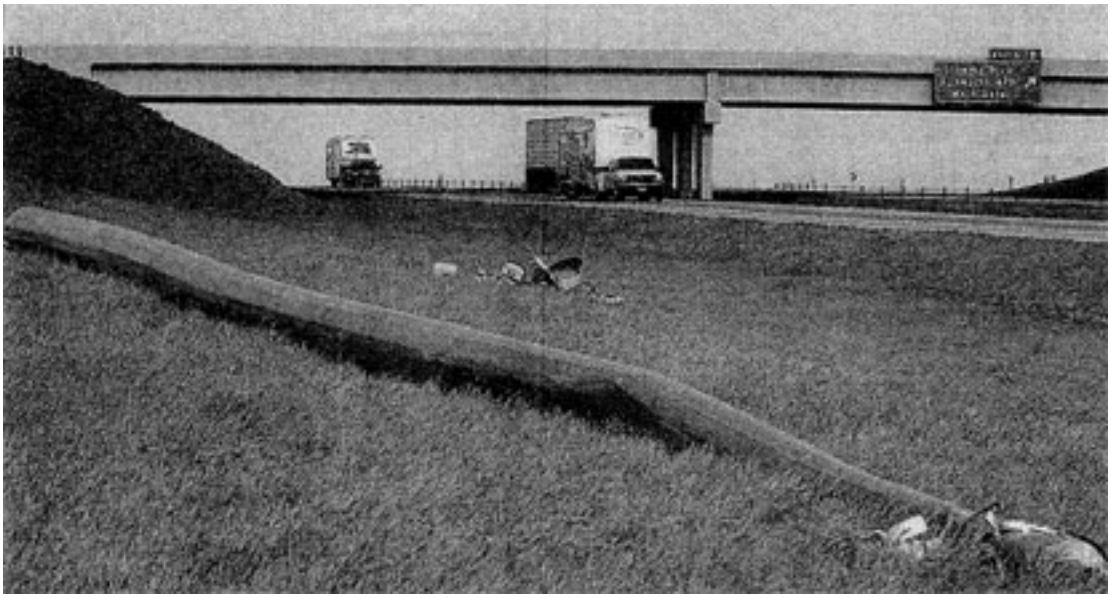

Figure 1.10: Failure of high mast lighting tower in Rapid City, South Dakota (Courtesy of Rapid City Journal)

A common characteristic that the two failures in Rapid City, SD had was both poles fractured just above the pole to base plate weld; leaving the base plate completely intact. This can be seen in Figure 1.11. Note that the pole wall remaining inside of the base plate socket is visible. Failure of the structure at the toe of a structural weld indicates a fatigue type failure.

Figure 1.11: Remaining intact base plate in South Dakota (Courtesy of Rapid City Journal)

Figure 1.12 shows another high-mast lighting tower failure in Colorado that occurred in February of 2007. Similar to the failure in South Dakota, fracture initiated at the weld toe in the base plate to pole wall connection, and then propagated around the pole wall until the structure collapsed. It should be noted that a common trait in these two high-mast lighting tower failures is that both used a relatively thin base plate (less than 2-in).

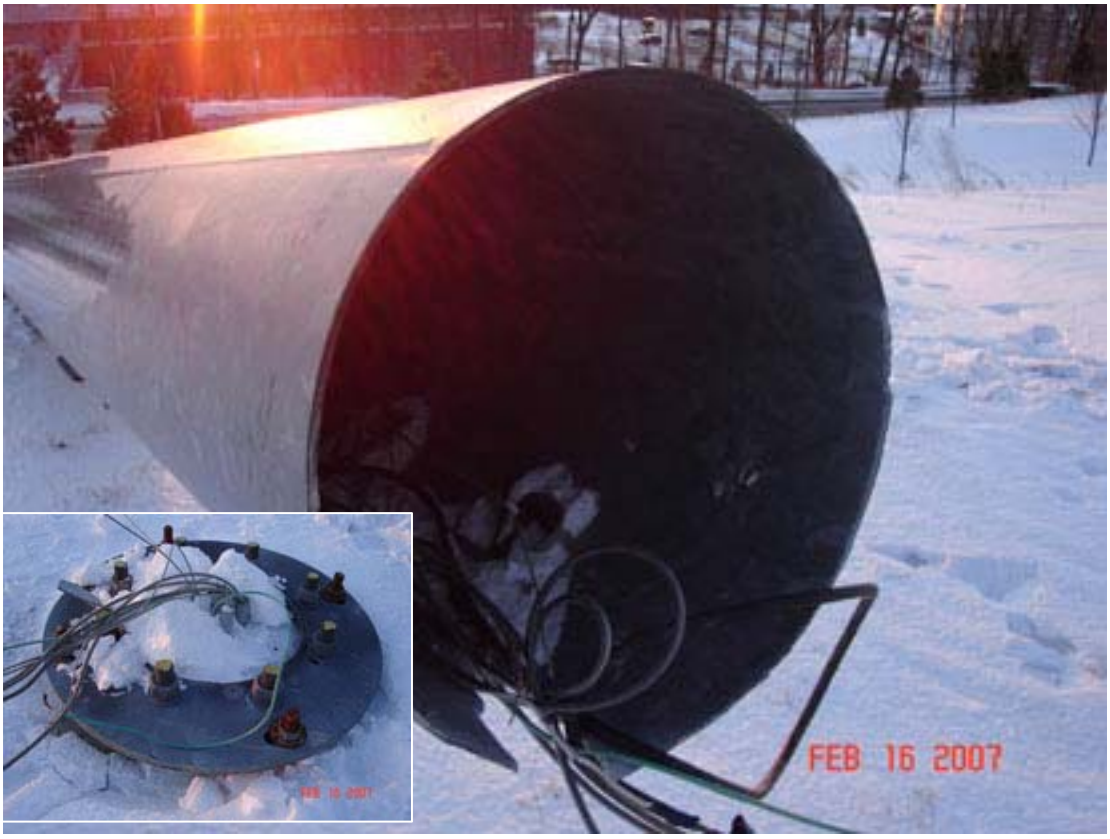

Figure 1.12: Failure in Colorado

1.5 HIGH MAST LIGHTING TOWER DESIGN USING AASHTO

The design of high-mast lighting towers is governed by AASHTO Standard Specifications for Structural Supports for Highway Signs, Luminaries and Traffic Signals (AASHTO, 2001). Section 11 of the AASHTO Specification contains provisions for the fatigue design of cantilevered structural supports. This section is based on NCHRP Report 412, *Fatigue Resistant Design of Cantilevered Signal, Sign and Light Supports* (Kaczinski et al., 1998).

Fatigue design for high-mast lighting towers is based on an *infinite-life* fatigue approach. In this approach, the stresses due to equivalent static load effects must remain below the constant-amplitude fatigue limit (CAFL). The stresses are modified by an importance factor given in Section 11.6 of the AASHTO Specification. These importance factors are based on the degree of hazard to traffic and damage to property,

should the structure fail. The *infinite-life* fatigue approach can be used when the number of wind load cycles expected during the lifetime of the structure is greater than the number of cycles at the CAFL (AASHTO, 2001).

It is important to note that in the AASHTO Specification there are no regulations regarding the geometry of the connection. The findings of this research, as well as previous research shows that variables such as base plate thickness and number of bolts used in the base plate has a significant effect on the fatigue resistance of the structure.

1.6 RELATED RESEARCH

1.6.1 Physical Testing

No known physical testing has been performed on the fatigue resistance of high-mast lighting towers. However, there has been extensive physical testing on similar traffic structures that utilize connection details similar to those used in the high-mast poles; those traffic structures being horizontal traffic signal mast-arms. Valuable information was learned in the physical testing of the smaller diameter horizontal mast-arms that could be applied to the design of the larger diameter high-mast lighting poles.

Fatigue in traffic signal mast-arms was first studied at Lehigh University in 1983. The research performed at Lehigh showed that the typical socketed connection used in horizontal mast arms performed worse than a Category E' detail when using an equal leg fillet weld and a Category E when using an unequal leg fillet weld. The improved performance of the unequal leg fillet weld over the equal leg fillet weld was attributed to the reduction in contact angle at the weld toe. As a result of the testing performed in this study, the unequal leg fillet weld became the standard weld utilized in the socketed connection detail (Miki, 1984).

Experimental research was performed on wind loading, dynamic response, and fatigue of cantilevered sign, signal, and luminary support structures by Kaczinski et al. and documented in NCHRP Report 412. As mentioned previously, the purpose of this report was to develop guidelines for the design of cantilevered traffic structures in fatigue. The guidelines reported were used to update the AASHTO design specifications

by developing and evaluating the existing static wind loads due to vortex shedding and galloping (Kaczinski et al., 1998).

Extensive testing was conducted by the University of Texas to evaluate the fatigue categorization of typical connection details as well as evaluate the design methodology for stiffened connection details. An investigation of the effectiveness of Ultrasonic Impact Treatment on welds was also performed. The results of the research confirmed the classification of the unequal led fillet welded socket connection as a Category E' detail. It was also found that socketed connections with 2-in base plates exhibited a significant improvement in fatigue life when compared to specimens with a 1.5-in thick base plate. The UIT treatment procedure was found to be most effective when galvanizing the pole prior treatment. In addition, the U-Rib stiffened connection exhibited an improved fatigue life when compared to the socketed connection detail (Koenigs, 2003).

1.6.2 Analytical Modeling

Although there is a lack of physical testing on the high-mast lighting towers, analytical studies such as finite element analyses have been performed on the traffic structures.

An analytical study investigating the effect of base connection geometry on the base plate flexibility and fatigue performance of high-mast lighting towers was performed at Lehigh University. The study showed that base plate flexibility has a considerable influence on the stress behavior in the pole wall in the socketed connection. Parametric studies performed in the research showed that the major influence of base plate flexibility is the base plate thickness and the most cost effective way to decrease flexibility of the base plate is to increase the thickness. A minimum base plate thickness of 3-in and a minimum pole wall thickness in the lower section of the tower be 1/2-in (Warpinski, 2006).

Similar to work performed at the University of Texas, a parametric study was performed at the University of Minnesota using finite element analysis to examine how the stress concentration factor (SCF) changes with connection geometry in socketed

connections (Koenigs et al, 2003; Ocel, 2006). In total, 222 models were analyzed which varied connection geometries such as pole wall thickness, pole diameter, bend radius in multi-sided shapes, and base plate thickness. It was found that the stress concentration factors in multi-sided poles such as those used in high-mast lighting towers increases when using fewer anchor rods and using sharper tube bends. It was also found that the SCF decreases exponentially by increasing the base plate thickness (Ocel, 2006).

1.7 SCOPE

The objective of this research was to evaluate the fatigue performance of typical fatigue critical connection details used in high-mast lighting towers. Laboratory fatigue testing was performed on full-scale specimens utilizing fillet welded socket connections, full penetration weld connections, as well as a stool base connection detail. The investigation addressed several issues concerning the fatigue characteristics of high mast lighting poles. These issues included: 1) The influence of base plate thickness on the performance of socketed connections 2) The influence of the number of anchor bolts used in base plates 3) The performance of a full penetration weld compared to a fillet welded socket connection when using a 2-in base plate 4) The evaluation of fatigue performance of the anchor bolt stool connection in high-mast lighting poles similar to those used in the state of Iowa.

The following chapters discuss the results of this testing program. The test specimen design and test setup are described in Chapters 2 and 3, respectively. Testing procedure is discussed in Chapter 4. The results of fatigue testing as well as material tensile tests and chemistry analysis are discussed in Chapter 5. Chapter 6 presents general conclusions from the test results, as well as recommendations for further research.

CHAPTER 2

Test Specimen Design

2.1 SPECIMEN DESIGN

The designs of typical high-mast lighting towers used by various states sponsoring this pooled fund study provided the guidelines for the design of test specimens used in this research. It was decided to test fillet welded socket connections, full penetration welded connections, as well as a stool base connection detail.

In order to remain consistent with details used in multiple states, a pole diameter of 24-in was chosen. A pole diameter of 24-in also allowed the use of a load range within the limits of the ram selected for the test setup that would produce the desired stress range in the poles.

The holes in the base plate were design to accommodate 1¾-in threaded rods and were oriented in a circular pattern with a circumference of 30-in. The outer diameter of the base plates was 36-in.

A pole taper of 0.14-in/ft was used for the specimens. This was recommended by Valmont Industries, the high-mast pole manufacturer supplying the test specimens, as common practice in the manufacturing of high-mast lighting towers. A common wall thickness of 5/16-in was used for all specimens. This pole wall thickness was also recommended by Valmont Industries as a common wall thickness used in this diameter pole.

The length of each specimen was governed by the test setup used which is described in Chapter 3. In order to facilitate testing at the desired load range and at a reasonable speed, the length of each specimen including the base plate, pole, and end reaction plate was 174¼-in or 14-ft 6¼-in. Figure 2.1 shows the fabrication drawing for the high-mast specimens.

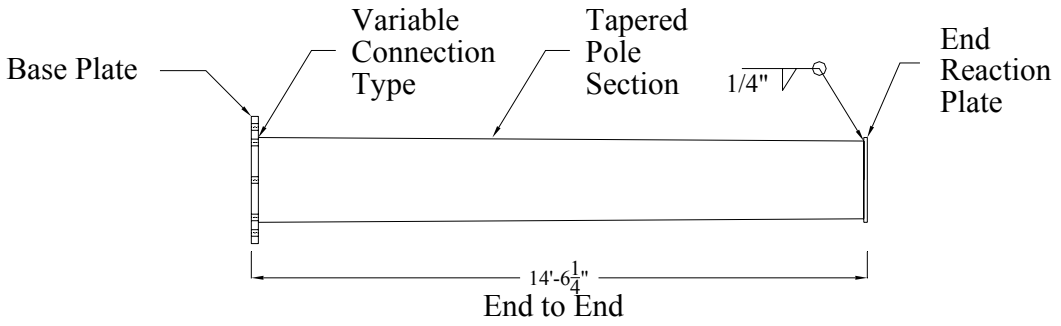

Figure 2.1: Test specimen fabrication drawing

All high-mast specimens were galvanized after fabrication. Previous research on horizontal mast-arms has shown that galvanizing has a detrimental effect on the fatigue life of the structures (Koenigs, 2003). Since most high-mast lighting towers are galvanized, it was decided by the sponsors to galvanize all test specimens in order to provide a measure of the fatigue life of lighting structures in use.

2.2 FILLET WELDED SOCKET CONNECTION

A common base plate to pole connection detail used in high-mast lighting towers is the fillet welded socket connection. In this connection detail, a hole is cut into the base plate, into which the pole section is inserted. A structural, unequal-leg fillet weld is then run on the outside of the pole wall connecting the pole to the base plate. A seal weld is then run on the edge of the pole wall inside of the base plate hole. The fillet welded socket connection and weld detail are shown in Figures 2.2 and 2.3, respectively.

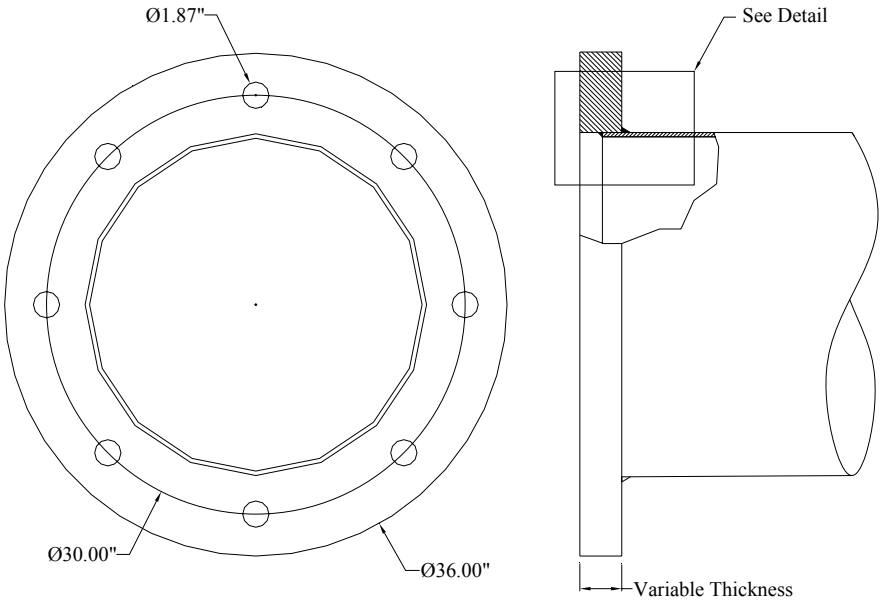

Figure 2.2: Fillet welded socket connection detail

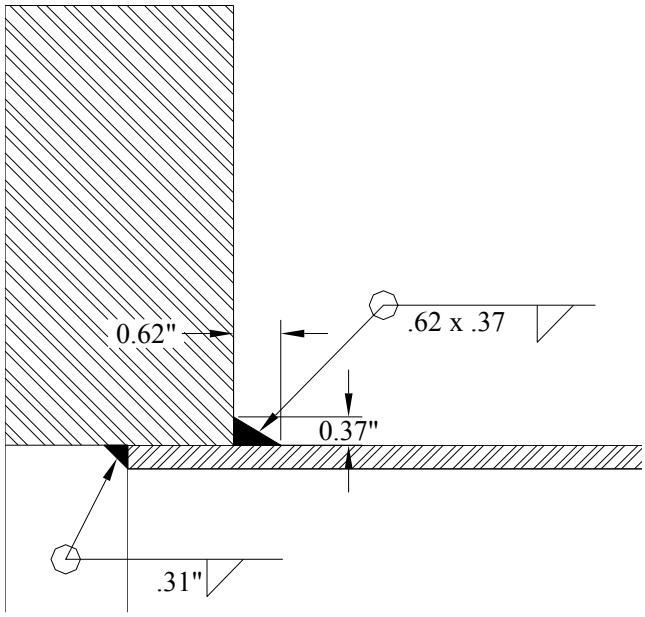

Figure 2.3: Socket connection weld detail

Figure 2.3 shows the weld detail used for the fillet welded socket connection. The weld detail uses a 0.62-in x 0.37-in unequal-leg fillet weld. These weld dimensions were determined using the design specification used in the state of Texas. A 0.31-in fillet seal weld is used at the edge of the pole wall to prevent corrosion and the entrapment of flux from the galvanizing bath in the gap between the pole wall and base plate and prevent the trapping of slag and acid from the galvanizing process in the gap.

Two bolt geometries were tested in this detail which included an 8-bolt and 12-bolt hole pattern. In addition, two base plate thicknesses were tested, 1 ½-in and 2-in.

2.3 FULL PENETRATION WELDED CONNECTIONS

Two variations of a full penetration weld connection were included in the testing program. One variation utilized a back-up bar similar to the design used in the state of Wyoming. The other detail did not use a back-up bar and was based upon the full penetration weld connections used in the state of Texas.

2.1.2 Wyoming Detail

In the state of Wyoming, a full penetration weld is used in high-mast lighting towers with a back up bar as shown in Figures 2.4 and 2.5. In this connection detail, the beveled pole wall is welded with a full penetration unequal-leg weld run on the outside of the pole wall.

As shown in Figure 2.5, the bevel at the edge of the pole wall is cut at a 45-degree angle. A 0.25-in root opening on the full penetration weld is used. Seal welds are used at both the top and bottom of the backing bar to prevent corrosion. All weld dimensions were determined from design specifications used in the state of Wyoming. The welded back up bar also acts as local reinforcement to the pole wall which reduces stress in at the weld toe (Koenigs, 2003).

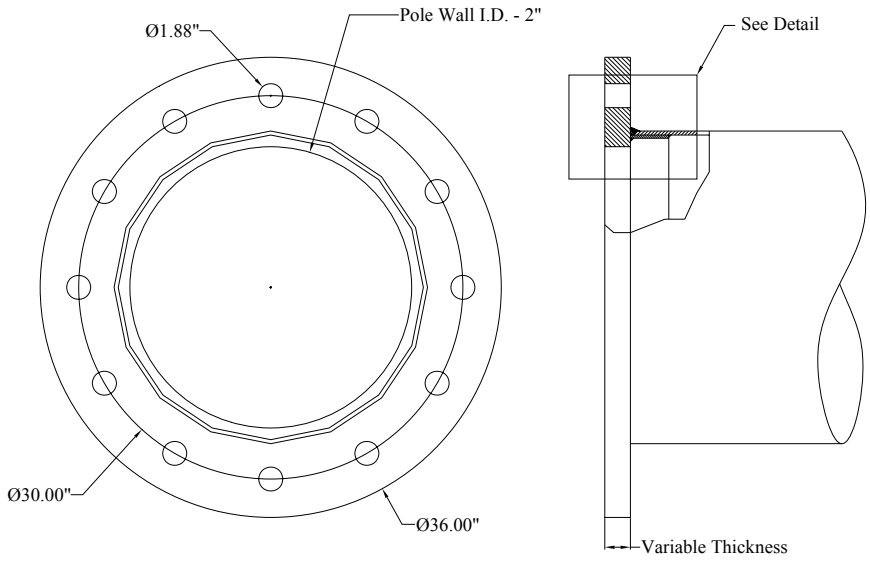

Figure 2.4: Wyoming connection detail

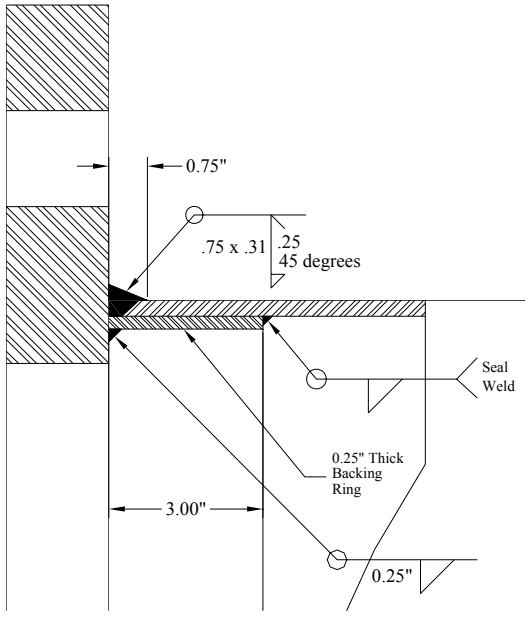

Figure 2.5: Wyoming connection weld detail

Note that the inside diameter of the base plate is 2-in less than the diameter of the pole wall. This base plate inside diameter was chosen by the manufacturer, Valmont Industries, to allow the welder to make the welds inside of the pole wall.

An 8-bolt hole pattern in conjunction with a 2-in base plate thickness was used for the Wyoming Detail.

2.1.3 Texas Detail

The full penetration weld in the Texas detail is similar to the one used in Wyoming, with the exception of the back up bar. The Texas detail does not use a back up bar in order to avoid the risk of acid entrapment between the pole wall and base plate during the galvanizing process. The pole wall is butted up against the base plate and a ¼-in. fillet weld is used to attach the inside of the pole to base plate. The ¼-in. fillet weld acts essentially as a backup for the full penetration unequal leg weld that is run on the outside of the pole. For similar reasons as the Wyoming detail, the inside diameter of the base plate is 2-in less than the diameter of the pole wall. All weld dimensions were determined using design specifications used in the state of Texas. A 12-bolt hole pattern in conjunction with a 3-in base plate was used for the Texas detail.

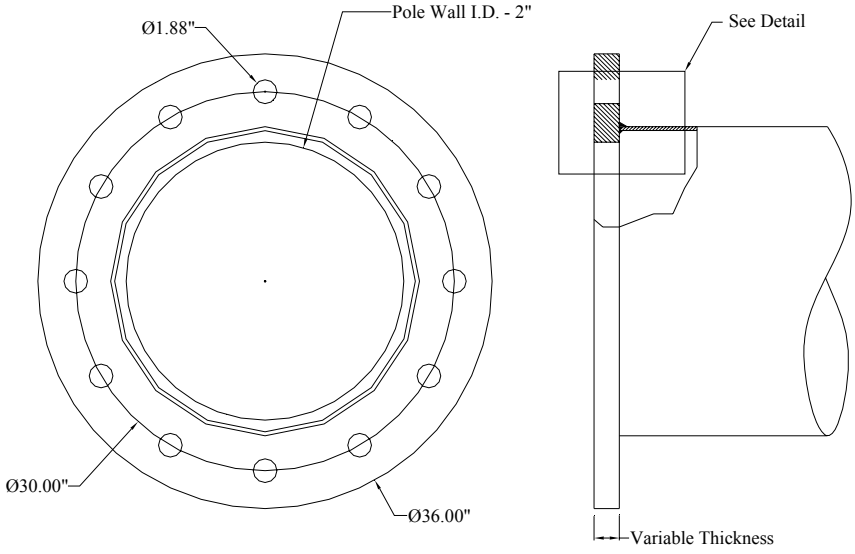

Figure 2.6: Texas connection detail

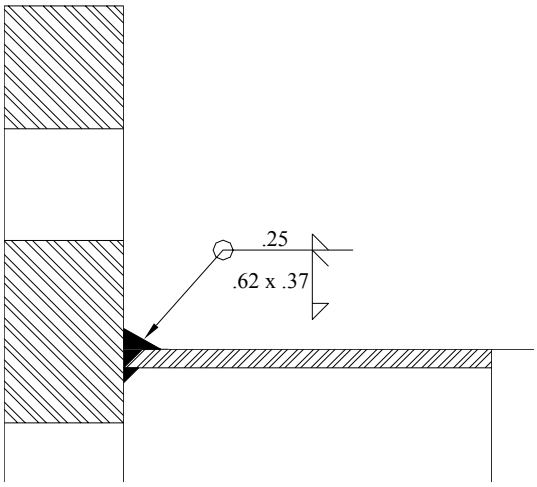

Figure 2.7: Texas connection weld detail

2.4 STOOL BASE DETAIL

The stool base detail was developed by the research team to replicate the U-Rib stiffener detail used in horizontal mast-arms and a similar detail used in early high-mast poles in Iowa. In horizontal mast-arms, the U-Rib connection detail showed significant improvement in fatigue life over fillet welded socket connections (Koenigs, 2003). The U-Rib connection can be seen in Figure 2.8.

Figure 2.8: U-Rib stiffened horizontal mast-arm

Rather than using a U-Rib stiffener on the high-mast lighting tower, vertical stiffener plates in conjunction with a cap plate were used as shown in Figures 2.9 and 2.10. In essence, the vertical plates along with the cap plate would have the same effect as the U-Rib stiffener in the horizontal mast arm. Having flat plates rather than a curved stiffener also simplifies fabrication.

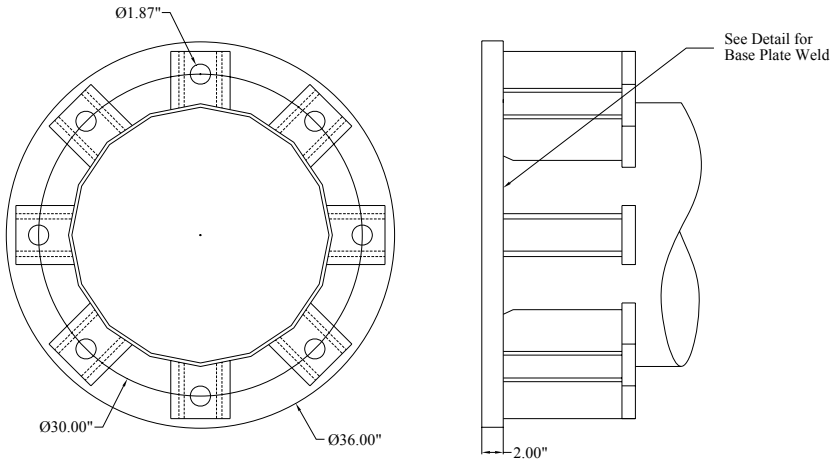

Figure 2.9: Stool base connection detail

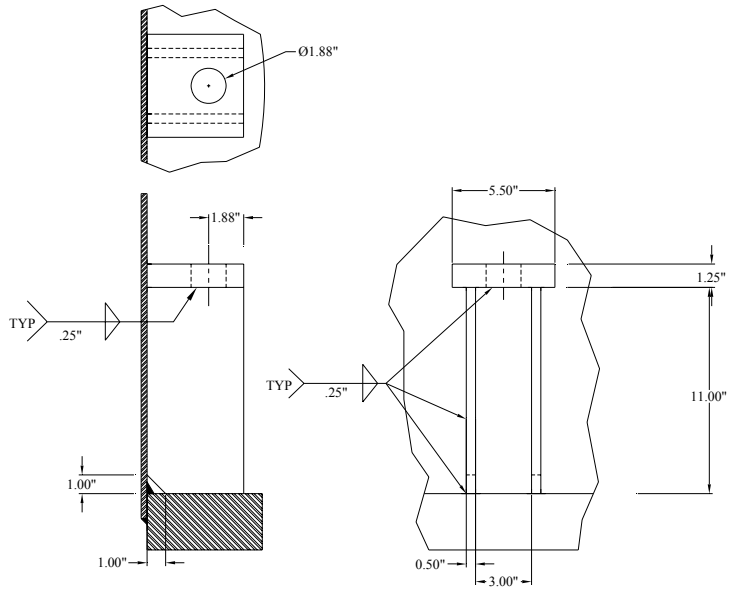

Figure 2.10: Stool chair detail

In fabrication, before the addition of the vertical plates and cap plate, the pole wall is connected to the base plate in the same manner as a fillet welded socket connection. The base plate to pole wall weld detail can be seen in Figure 2.11.

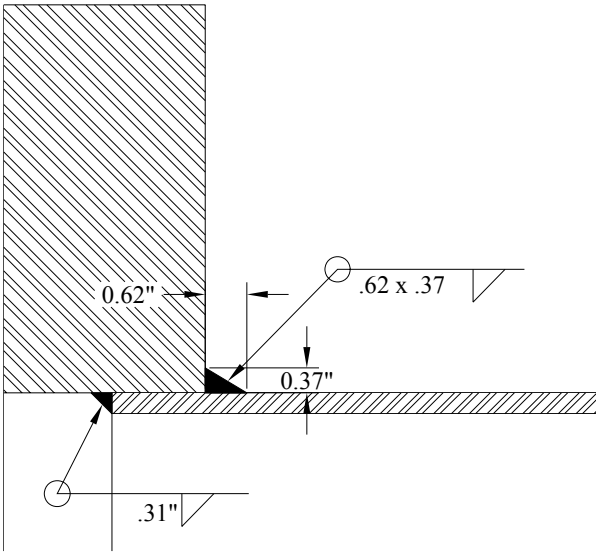

Figure 2.11: Base plate weld detail for stool base connection

2.4.1 Stool Base Stiffener Design

A relatively straightforward design approach was used for the sizing of the vertical stiffeners in the stool base detail. The stiffeners were designed to accommodate a force that would fully develop the yield strength of the anchor bolts as shown in the following calculations and in Figure 2.12.

Anchor Bolt:

$1\ \ 3/4"\phi$

$F_y = 105^{ksi}$

$A = 2.41\,\text{in}^2$

$P_y = F_y \times A = 252^{kips}$

Therefore: 252 kips will bear on cap plate resulting in 126 kips in each vertical stiffener.

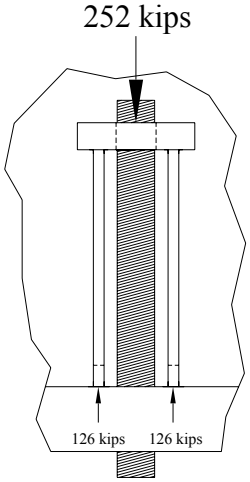

Figure 2.12: Free-body diagram for vertical stiffener plates

Required vertical stiffener width, w:

Gr. 50 Steel

Stiffener extends 5-in away from pole wall

$$F_y \times A = 126^{kips};\ A = 5'' \times w$$

$$w = \frac{126^{k}}{F_y \times 5''} = \frac{126^{k}}{50^{ksi} \times 5''} = 0.5''$$

Therefore: The required stiffener width is 0.5-in

Check local buckling in stiffener plates:

Note: conservative to neglect boundary conditions at cap and base plate.

$$f_{cr} = \frac{\pi^2 E}{12(1-\mu^2)}\left(\frac{t}{b}\right)^2 k$$

t = 0.5-in

b = 5-in

k = .763 (AISC LRFD 3rd ed.- Appendix B)

$$f_{cr} = \frac{\pi^2 \cdot 29000^{ksi}}{12 \cdot (1 - 0.3^2)} \left(\frac{0.5"}{5"} \right)^2 \cdot 0.763 = 200^{ksi}$$

$$f_{cr} > f_y$$

Therefore, local buckling does not control design

Size welds in vertical stiffeners:

Weld strength: $1.4 \frac{kips}{in \cdot \frac{1}{16}}$

$$126^{kips} \leq 1.4 \cdot S \cdot 2L$$

S = weld size in sixteenths of an inch

L = Length of weld (2L is used since both sides of plate will be welded)

$$\frac{126^{kips}}{1.4 \cdot 2} \leq S \cdot L$$

$$S \cdot L \geq 45$$

Assuming ¼-in fillet ($S = 4$):

$$L \geq \frac{45}{4}$$

$$L \geq 11\text{-}in$$

Therefore, vertical stiffeners must be 11-in in height.

2.5 TEST MATRIX

The test matrix was designed to investigate several variables and their effects on the fatigue life of the high-mast lighting towers. The variables included in the test matrix addressed several issues regarding the fatigue performance of the poles. These issues included:

1) The influence of base plate thickness on the performance of socket connections
2) The influence of the number of anchor bolts used in base plates

3) Comparison of the performance of a full penetration weld with the fillet welded socket connection when using a 2-in base plate

4) Comparison of Texas and Wyoming full penetration weld details

5) Evaluate the fatigue performance of the anchor bolt stool connection relative to the socket and full penetration weld connections

The testing matrix is shown in Table 2.1. Due to limitations on the number of specimens not all conditions could be tested for the full range of base plate thickness and number of anchor bolts.

Table 2.1: Test matrix for 24-in high mast poles

Base Plate Size	Weld Type	# of Specimens	
		8 Bolts	12 Bolts
1 1/2-in	Fillet	2	2
2-in	Fillet	2	2
	Full Pen.	2 (WY)	
2-in (with Stools)	Fillet	2	
3-in	Fillet	2	
	Full Pen.		2 (TX)

2.6 SPECIMEN LABELS

In order to easily identify specimens and their geometric properties, a unique labeling system was used. The first number in the label indicates the pole diameter. The base plate thickness and number of bolt holes used in the base plate are identified by the second and third numbers, respectively. The letters following the bolt hole number identify the connection type used in the specimen. The final letter indicates the individual specimen. This labeling system is illustrated in Figure 2.13.

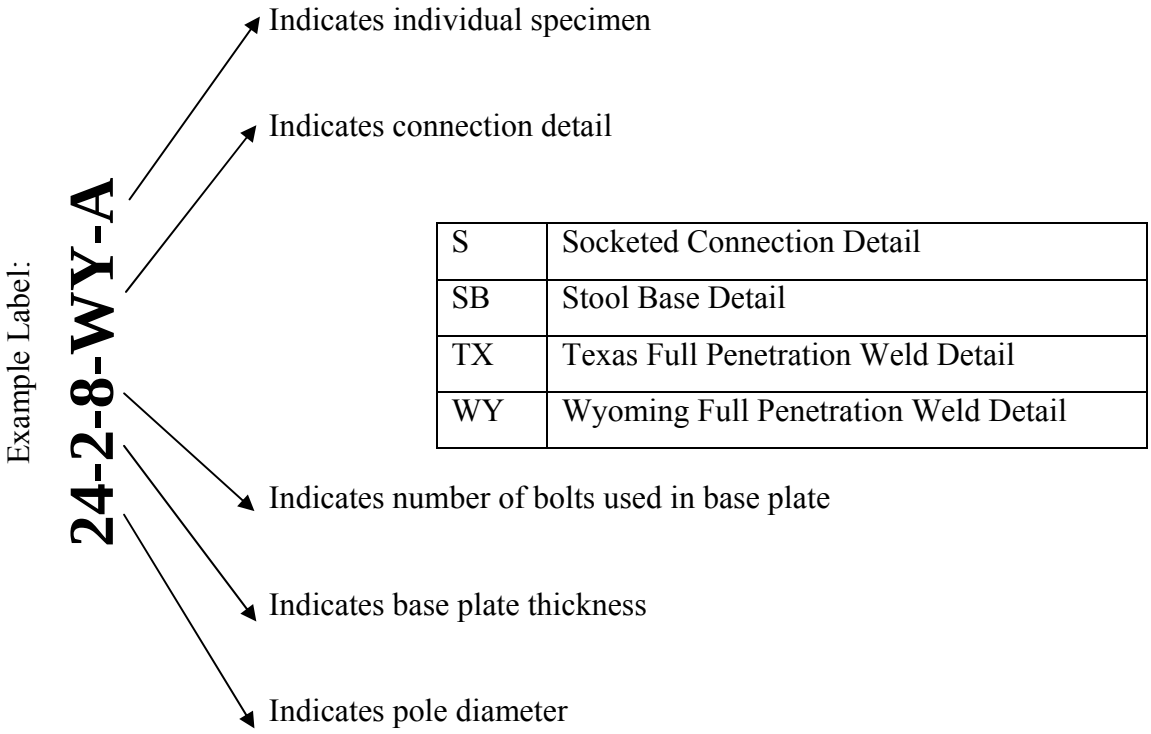

S	Socketed Connection Detail
SB	Stool Base Detail
TX	Texas Full Penetration Weld Detail
WY	Wyoming Full Penetration Weld Detail

Figure 2.13: Labeling system used for high-mast specimens

CHAPTER 3

Test Setup

3.1 DESIGN DECISIONS

Two test setup designs were considered for the testing of the high-mast pole specimens. The first option involved the testing of specimens in a vertical orientation with the base plate fixed to a reaction floor and the hydraulic actuator reacting against a reaction wall. A schematic of this test setup can be seen in Figure 3.1.

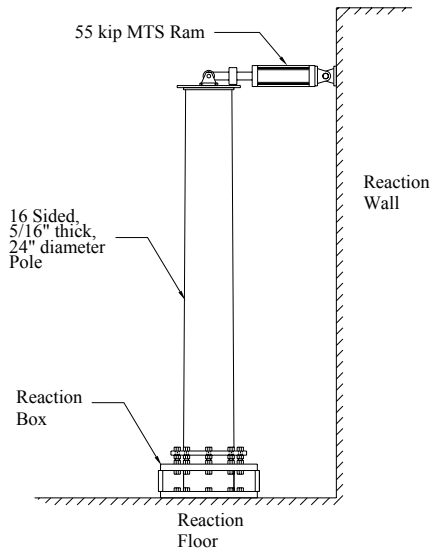

Figure 3.1: Vertical test setup option

An advantage of the vertical test setup is that stress reversal in the pole wall would be possible during testing. This would replicate field conditions since the pole oscillates about the vertical position when excited by the wind. However, in this test setup only one specimen at a time could be tested leading to a prolonged testing period.

Furthermore, installation of specimens would be difficult since the hydraulic actuator would have to be held in position while the pole is being installed.

The other test setup considered for the testing of the high-mast poles is very similar to the tension test setup used in the testing of horizontal mast-arms at the University of Texas (Koenigs, 2003). In this setup, two specimens are tested simultaneously and are coupled at the base plate using a loading box. The two specimens are essentially two cantilevers which form a simply supported beam; the hydraulic actuator applies an upward force creating a negative moment in the 'beam'. This test setup can is shown in Figure 3.2.

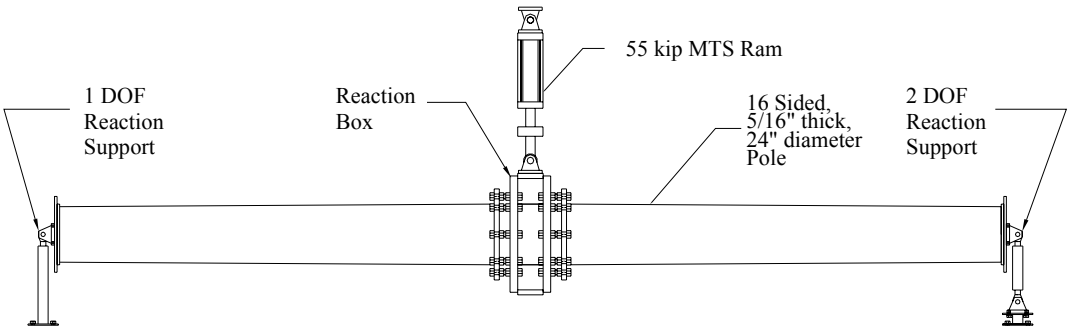

Figure 3.2: Tension test setup

A disadvantage of this test setup is that stress reversal is not possible since the system would be unstable because the hydraulic actuator has swivels at both ends and the 2 DOF support has similar end conditions. However, this test setup allows the testing of two specimens simultaneously which decreases overall testing time. Installation of specimens is easier since the loading box can be suspended by the hydraulic actuator while the specimens are bolted into place one at a time.

It was for these reasons that the tension test setup was chosen to test the high-mast lighting towers. A 55 kip capacity MTS hydraulic actuator was used in the test system and was controlled by an MTS FlexTest SE Controller. Hydraulic pressure was supplied by an MTS SilentFlo HPU operating at 3000 psi with a 90 gpm capacity. Hydraulic pressure was regulated by an MTS 293 Hydraulic Manifold.

3.2 TEST SETUP DESIGN

3.2.1 Test Setup Length

The test setup length (the distance between reaction supports) was an important issue during the design of the testing system. A long setup length would require less force from the hydraulic actuator, but would require more stroke from the ram; hence, requiring more hydraulic fluid flow. Conversely, a shorter test setup would require a smaller stroke and less hydraulic fluid flow, but would require more force from the hydraulic actuator. In order to determine the most efficient test setup length, several models of the test setup were created with various lengths using SAP2000. The SAP models were used to estimate deflections at maximum and minimum desired stress levels. These maximum and minimum stress deflections would give the required ram stroke for a specific test setup length; which, in turn, would give the required hydraulic oil flow.

In order to provide a finite fatigue life, it was decided that the nominal bending stress range at the base plate to pole connection weld would be 12 ksi. The required moment range needed in the 'beam' is given by the following equation:

$$M_R = \frac{S_R \cdot I}{c}$$

Where: M_R is the required moment range
S_R is the required stress range
I is the moment of inertia of the pole section
c is the distance from the centroid to extreme fiber

The moment of inertia of the 24-in diameter pole section, idealized as a round section, is given by the following equation:

$$I = \frac{1}{4}\pi\left(r_0^4 - r_i^4\right) = \frac{1}{4}\pi\left(12^4 - (12 - 5/16)^4\right) = 1631.34 in^4$$

In order to determine the required load at mid-span in each SAP model, the moment at the base plate to pole weld was calculated using the equation below:

$$M_R = \left(\frac{14.67}{16}\right) \cdot \frac{P_R \cdot L}{4}$$

Where: P_R is the required load for a given test setup length

Note that in the equation there is a ratio of 14.67/16. This is due to the fact that the desired stress range of 12 ksi does not occur at mid-span of the simply supported beam, but rather, at some distance offset from center at the pole to base plate connection weld. This distance was assumed to be 16-in for the purposes of the SAP model; hence, the value of 14.67 in the moment ratio.

Test setup lengths of 24-ft, 32-ft, and 40-ft were modeled using SAP2000. Note that the length of setup is restricted to 8-ft increments due to the spacing of tie down holes in the reaction floor at Ferguson Structural Engineering Laboratory. In order to replicate the taper of the pole specimen of .14 in/ft, the poles in the SAP model were broken into 6-in segments with varying outside diameters. The loading box was assumed as a rigid element. This SAP model is illustrated in Figure 3.3.

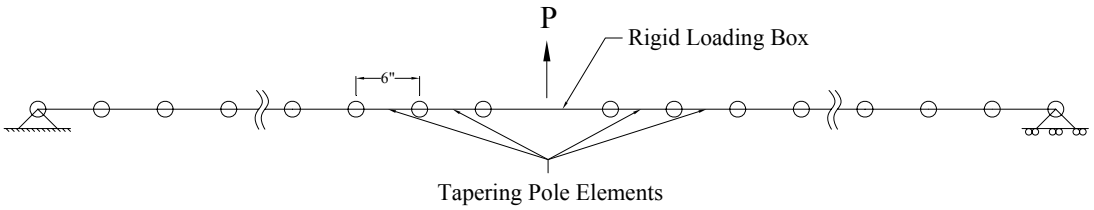

Figure 3.3: Illustration of SAP model

Table 3.1 shows the results from the SAP analysis models.

Table 3.1: Stress and deflections from SAP

L (ft)	Specimen Length (in)	At Maximum Deflection				
		Required Load (Kips)	Moment at Base Plate (K-in)	Max Stress at Base Plate (Ksi)	Deflection at Stress of	
24	134	43.98	2990.79	22	0.843	
32	182	32.51	2990.79	22	1.355	
40	230	25.78	2990.79	22	1.98	
L (ft)	Specimen Length (in)	At Minimum Deflection				Stroke Required (in)
		Required Load (Kips)	Moment at Base Plate (K-in)	Max Stress at Base Plate (Ksi)	Deflection at Stress of	
24	134	19.99	1359.45	10	0.471	0.372
32	182	14.78	1359.45	10	0.7448	0.610
40	230	11.72	1359.45	10	1.0688	0.911

Once the required ram stroke for each setup length was determined from SAP, the required hydraulic oil flow was computed using the following equations:

$$V_{oil} = A_{ram} \cdot S_{ram}$$

Where: V_{oil} is the volume of oil required on each stroke

A_{ram} is the ram piston area = $13 in^2$

S_{ram} is the required stroke for the setup length

$$Flow = V_{oil} \cdot Testing\ Speed$$

Table 3.2 shows the calculated flows required for each setup length.

Table 3.2: Required Flow Calculations

L (ft)	V_{oil} Required (in^3)	Testing Speed (Hz)	Flow, Q_{req} (in^3/s)	Flow, Q_{req} (gpm)
24	4.836	2	9.67	2.51
32	7.9326	2	15.87	4.12
40	11.8456	2	23.69	6.15

The flow requirements for all test setup lengths were within the limits of the testing system. However, it was noticed that the required load to produce the maximum stress for the 24-ft setup, 43.98-kip, was fairly close to the capacity of the hydraulic actuator. If

the dead load of the specimens and loading box which was estimated to be 10 to 12 kips is added to this load, the capacity of the actuator would be exceeded. The shortest setup length that could be used was 32-ft.

3.2.2 Design of Loading Box

The loading box needed to be as close to rigid as possible to minimize its effect upon the distribution of the bolt forces in the specimens which in turn could influence the fatigue performance of the specimens. The box was designed using 3-in steel plate. The overall dimensions of the box were 46-in by 46-in by 16-in. The face of the loading box was designed to accommodate the 30-in diameter bolt-hole pattern of the high mast specimens being tested as well as a 36-in diameter bolt-hole pattern if future testing warrants a larger pole diameter. Rigidity of the box was further increased with the addition of a 3-in thick internal vertical stiffener. Fabrication drawings of the loading box are shown in Figure 3.4. All of the plates used were 3-in thick.

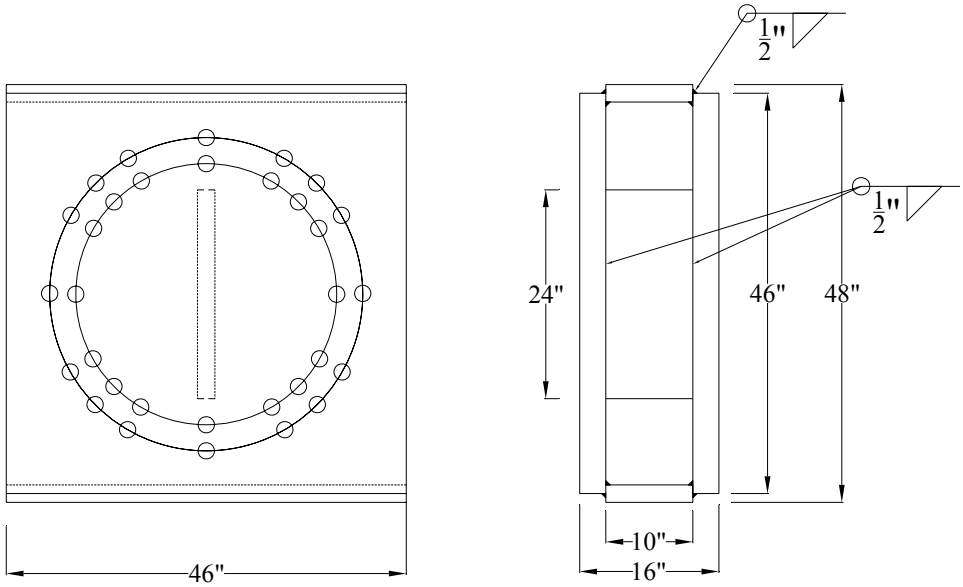

Figure 3.4: Fabrication drawing of loading box

In previous testing of smaller horizontal mast-arms at the University of Texas, washers were placed in between the base plate and the loading box to eliminate the possibility of a warped base plate from introducing uneven loading of the specimen (Koenigs, 2003). For this same reason, leveling nuts were used for the 24-in high-masts in this research. In addition to eliminating unwanted stresses, the leveling nuts also replicate field conditions as described in Chapter 1. The leveling nuts can be seen in Figure 3.5 below. Note that this picture was taken during installation and the specimen is not yet bolted to the loading box. The anchor rods were attached to the loading box by nuts on each side of the vertical side plates and then leveling nuts were used against the bottom of the specimen base plates. Additional nuts were used on what would be the top side of the base plate to complete the connection to the base plate. A star pattern was used in the tightening of the nuts to reduce the possibility of uneven tightening.

Figure 3.5: Leveling nuts used for base plate to loading box connection

3.2.3 Dynamic Analysis of Test Setup

Due to the large size and mass of both the loading box and high-mast specimens, a dynamic analysis of the testing system was performed. The dynamic analysis would determine if the testing speed desired would approach the natural frequency of the setup. Resonance in the system would make it difficult for the MTS controller to regulate displacements during testing. The dynamic analysis was simplified by assuming a single degree of freedom system as shown in Figure 3.6.

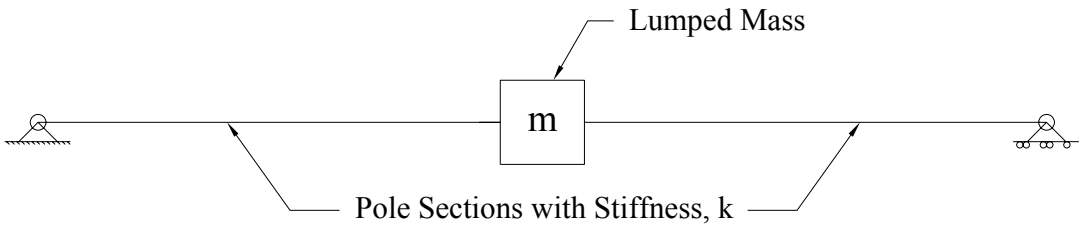

Figure 3.6: Single degree of freedom system used for dynamic analysis

The mass of the loading box and the two high-mast specimens is 'lumped' in the center of the system for ease of calculation. The dynamic analysis of the system is shown in the following calculations:

Assume: ξ (damping ratio) $\approx 1\%$

$k \approx 39$ kip/in (determined from SAP model)

Total weight of 3-in plate box and two specimens, $W = 8.6$ kips

$$m = \frac{W}{g} = \frac{8.6^{kip}}{386\frac{in}{s}} = .02228\frac{k-\sec^2}{in}$$

$$w_n = \sqrt{\frac{k}{m}} = \sqrt{\frac{39\frac{kip}{in}}{.02228\frac{k-\sec^2}{in}}} = 41.883\sec^{-1}$$

$$w_D = w_n\sqrt{1-\xi^2} = 41.883\sec^{-1}\sqrt{1-.01^2} = 41.83\sec^{-1}$$

$$f_n = \frac{w_D}{2\pi} = \frac{41.83\sec^{-1}}{2\pi} = 6.65Hz$$

The desired testing speed was 2 Hz to 4 Hz. Therefore, resonance was not an issue during testing.

3.2.4 Design of Reaction Supports

As mentioned previously, a simply supported beam analogy was used for the design of the test setup for the high-mast lighting poles. The reaction support shown in Figure 3.7 represents the pinned connection. The single degree of freedom reaction support restricts any lateral or vertical displacement and allows only rotation. The reaction support consists of a 4-in round riser, a spherical rod eye, clevis bracket, and a 1-in plate used to mate the reaction support to the end plate of the high-mast specimen.

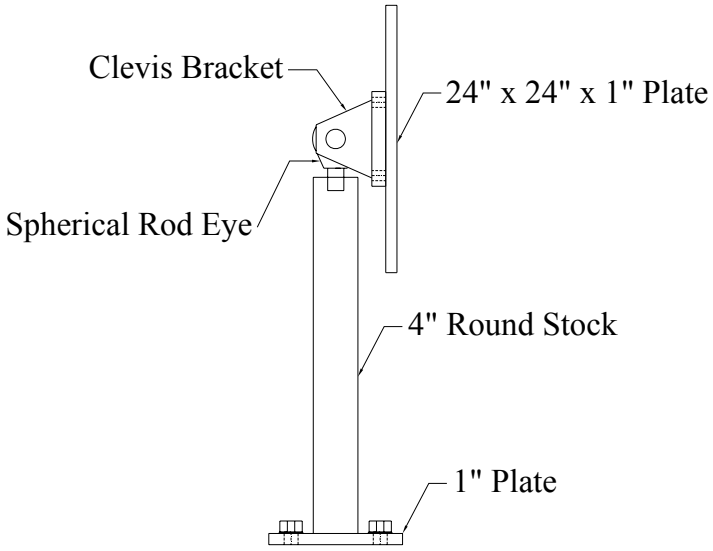

Figure 3.7: 1 Degree of freedom reaction support

The reaction support shown in Figure 3.8 represents a roller support in the simply supported beam analogy. While restricting vertical displacement, the reaction support allows lateral displacement as well as rotation much like a roller. The roller reaction support consist of a 5-in tall riser, 4-in round stock, two clevis brackets, two spherical rod eyes, and a 1-in mating plate. The 5-in riser was needed to provide clearance for the clevis bracket bolts since the bolt holes on the clevis bracket coincided with the bolt holes on the reaction floor but were or different diameters.

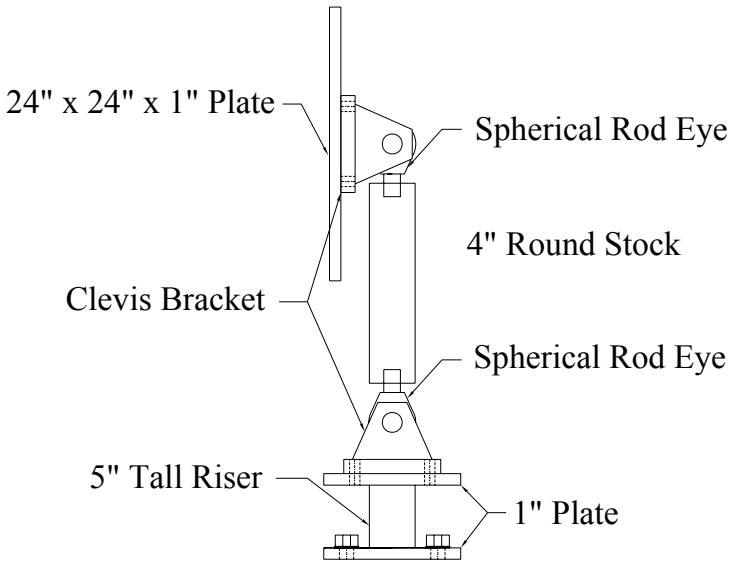

Figure 3.8: 2 degree of freedom reaction support

3.2.5 Portal Loading Frame

The 55-kip hydraulic actuator was attached to a portal frame with a single cross member as shown in Figure 3.9. The cross member height is adjustable. In order to accommodate the height of the actuator, the cross member needed to be relatively high on the frame. Diagonal bracing was needed to increase the out of plane stiffness of the frame to limit movement under dynamic loading.

Figure 3.9: Portal loading frame showing lateral bracing

3.3 MTS CLOSED LOOP SYSTEM

One may be deceived it is possible to simply enter loads or displacements into the controller, and the hydraulic actuator will cycle between those given values with minimal error. However, this may not be the case when testing cyclically. In a closed loop control system, such as the one used in the test setup, an analogue control signal is sent to the hydraulic actuator which controls the servo valves in the actuator. A feedback signal is then sent back to the controller telling the controller how the actuator is actually responding to the control signal. When testing cyclically, an error may be present between the command signal and the feedback signal. At lower frequencies, the error level is usually small as the feedback tracks the command signal more closely as shown in Figure 3.10. At higher frequencies, the error level becomes larger due to the phase lag as shown in Figure 3.11 (MTS, 2004).

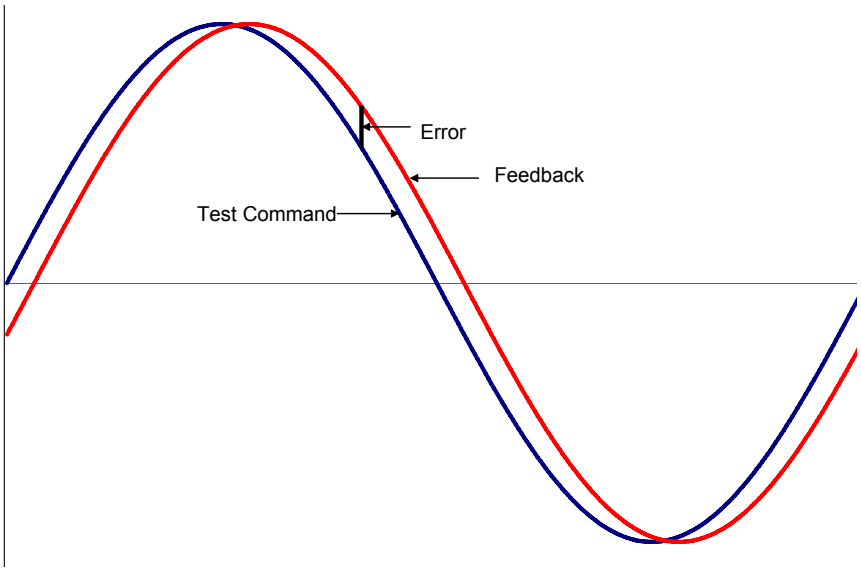

Figure 3.10: Error during low frequency cyclic testing

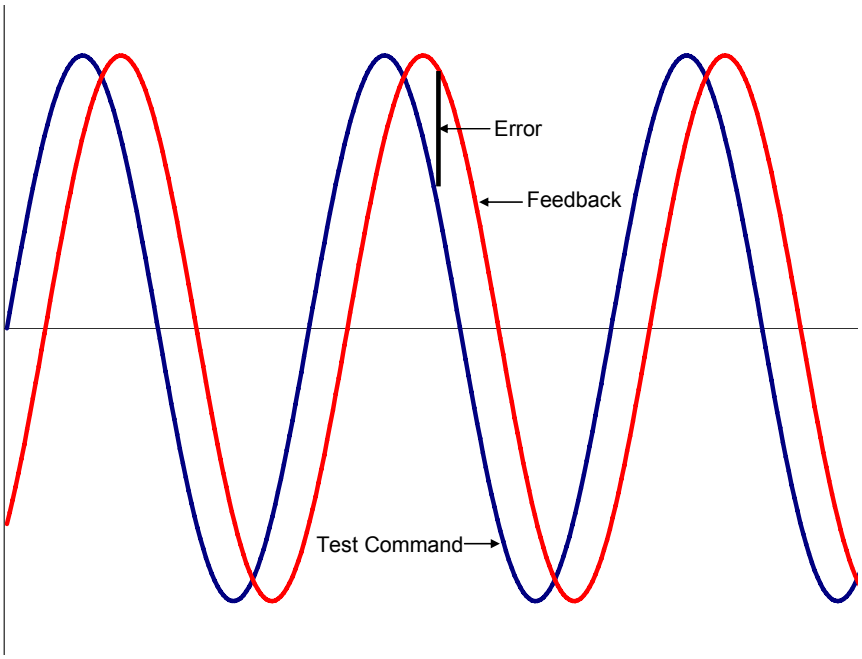

Figure 3.11: Error during high frequency cyclic testing

A valuable tool used during testing that the MTS FlexTest SE controller has is a Peak Valley Control (PVC) compensator. The PVC compensator monitors the sensor feedback

to ensure the command is properly applied to the specimens to achieve the desired loads or displacements. When the command is not properly applied and error becomes larger than acceptable, the compensator will adjust the analogue command signal to reduce the error between the command and feedback signals (MTS, 2004).

CHAPTER 4

Testing Procedure

4.1 GENERAL TEST PROCEDURE

All tests of the high-mast lighting poles were performed using the procedure described in this chapter. The testing procedure included specimen measurements, installation of the high-mast specimens, calculation of loads, and setting deflections under displacement control.

4.1.1 Specimen Measurements

Prior to specimen installation and testing, measurements were taken to determine dimensions in order to calculate the section properties of the specimens and document the weld geometry. These measurements included: base plate thickness, pole inside diameter at the base (both to flats of polygonal shape as well as to corners), pole inside diameter 12-in away from the base, pole wall thickness, and weld dimensions. Pole wall thickness was measured using a Krautkramer USN 60 ultrasonic detector and weld dimensions were measured with an adjustable fillet weld G.A.L. gage. In order to verify measurement obtained using the ultrasonic detector, measurements of thickness from three steel coupons were taken using a micrometer. The results are shown in Table 4.1. It was found that thicknesses taken using ultrasonic detection were within 3% of the true value.

Table 4.1: Verification of ultrasonic thickness measurements

Specimen	Thickness using micrometer (in)	Thickness using UT (in)	% Difference
24-3-12-TX-B	0.322	0.331	2.8
24-2-8-WY-A	0.337	0.342	1.5
24-2-8-S-B	0.329	0.337	2.4

The measurements for each test specimen are presented in tabular form in Appendix A.

4.1.2 Specimen Installation Procedure

Due to the relatively large size of the test specimens and the availability of only one overhead crane, a unique installation procedure was used for the high-mast lighting towers. The following outline describes the specimen installation procedure:

1. In order to remove the failed specimens, the hydraulic actuator was moved to a displacement at which zero-load was shown on the load cell of the actuator. At this displacement, the actuator was carrying the tared load which consisted of the weight of the loading box and two specimens. The reaction support pins could then be taken out; releasing the pole specimens from the supports as shown in Figure 4.1. A temporary support was inserted under the loading box and the closed loop control system was turned off.

Figure 4.1: Pole specimens released from reaction supports

2. The red end-reaction plates such as the one shown in Figure 4.1 were then transferred to the new pole specimens using an overhead crane as shown in Figure 4.2.

Figure 4.2: Transfer of reaction plates to new specimens

3. With one end supported by wooden blocks, the opposing specimen was then removed using the overhead crane; followed by the removal of the remaining specimen. It was important to support the opposing end before the removal of the first specimen to avoid an unbalanced load. Without supporting the opposing end, the remaining specimen would fall to the floor and tilt the loading box making it difficult to remove the first specimen.
4. A new pole specimen was then installed into the setup; wooden blocks were placed underneath the pole end before the crane was detached from the specimen to avoid an unbalanced load.
5. The remaining pole specimen was then installed.

6. The pole base plates were then leveled with respect to the loading box using the leveling nuts described in Section 3.2.2. A typical spacing of 4 ¼ -in was used between the base plate and loading box.
7. The nuts were then tightened using a 4-lb sledge hammer and slugger wrench. A star pattern was used in the tightening of the nuts to reduce the possibility of uneven tightening.
8. With the loading box and two specimens suspended by the hydraulic actuator, the load cell was zeroed.
9. The reaction support pins were then replaced, and the setup was ready to begin a new test.

4.1.3 Calculation of Loads

Using the measurements obtained from the specimens, the loads required to reach the minimum stress level of 10-ksi and a maximum stress level of 22-ksi at the face of base plate were calculated. The minimum and maximum loads were calculated based on the simply supported beam analogy illustrated in Figure 4.3:

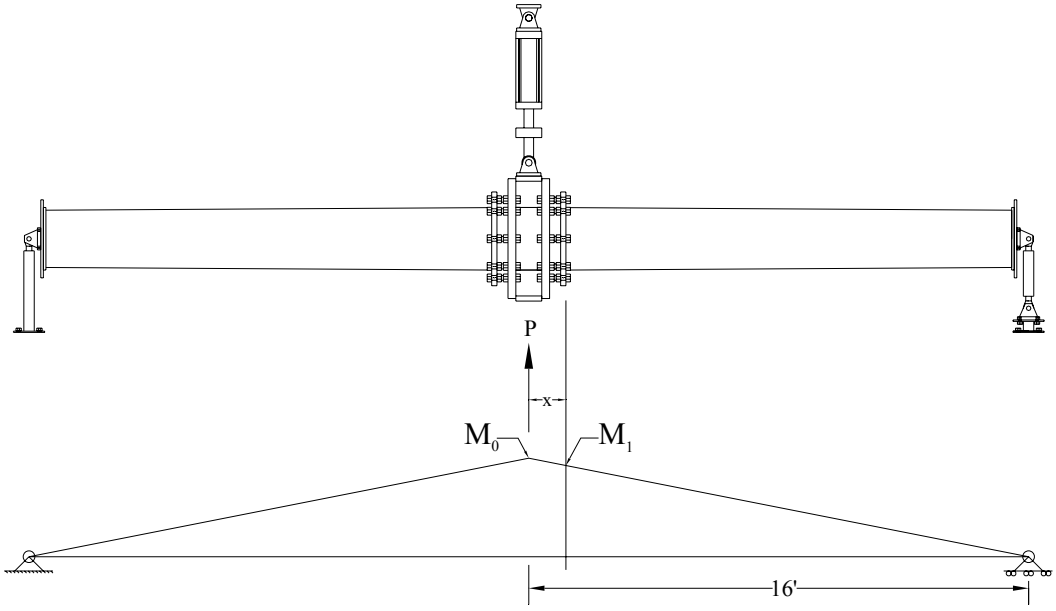

Figure 4.3: Moment diagram for calculation of stresses

The required load to reach either the minimum or maximum stress level was back calculated using the following equations:

$$\sigma_{req} = \frac{M_1 c}{I} \qquad c \text{ and } I \text{ determined from AutoCAD}$$

$$M_1 = \frac{16 - x}{16} \cdot M_0 \qquad \text{Note : x varies based on base plate thickness}$$

$$\mathrm{M_0} = \frac{16}{16 - \mathrm{x}} \mathrm{M_1} = \frac{16}{16 - \mathrm{x}} \sigma_{\mathrm{req}} \frac{\mathrm{I}}{\mathrm{c}}$$

$$M_0 = \frac{P_{req} \cdot L}{4} \qquad L = 32\,ft$$

$$P_{req} = \frac{M_0 \cdot 4}{L}$$

An accurate value for the moment of inertia of each pole section was obtained through the use of the "massprop" function in AutoCAD 2006. Using the measurements obtained from the pole specimens, the specimen cross sections were drawn in AutoCAD. Once drawn in AutoCAD, the "massprop" function would output the moment of inertia of the given cross section. This was very useful due to the polygonal shape of the pole cross section.

A spreadsheet was developed that would take the measurements from the pole sections and the moment of moment of inertias obtained from AutoCAD and calculate the required minimum and maximum actuator loads. A screenshot of the spreadsheet used for these calculations can be seen in Figure 4.4. The calculated loads for each test specimen can be found in Appendix B.

Specimen Names: **24-3-12-TX-A,B**

Specimen Dimensions

Test Length,L (ft):	32

Speciment A

Distance to weld from center,x (in):	15.3125
Ave. Pole **Inside** Diameter to Flats (in):	23.375
Ave. wall Thickness (in):	0.328

Specimen B

Distance to weld from center,x (in):	15.3125
Ave. pole **Inside** Diameter to Flats (in):	23.5625
Ave. wall Thickness (in):	0.331

Average

Distance to weld from center,x (in):	15.313
Ave. pole **Inside** Diameter to Flats (in):	23.469
Ave. wall Thickness (in):	0.330

Dimensions for use in AutoCad

Radius for Inside Circumscribed Circle (in):	11.734
Radius for Outside Circumscribed Circle (in):	12.064
Inside Bend Radii (in):	4.000
Outside Bend Radii (in):	4.330

Calculated Properties From AutoCad:

I (in^4) =	1784.095	1811.877 (using a circle)
C (in) =	12.216	

Desired Stresses:

σ_{min} (ksi) =	10
σ_{max} (ksi) =	22
σ_{mean} (ksi) =	16
stress range (ksi) =	12

Calculated Loads:

P_{min} (kips) =	16.532
P_{max} (kips) =	36.371

Figure 4.4: Spreadsheet used for calculation of testing loads

4.1.4 Setting Deflections under Displacement Control

Fatigue testing was conducted under displacement control. In order to determine the displacements that would correspond to the desired stresses at the connection, the setup was manually cycled under displacement control between the minimum and maximum calculated loads. When the displacements required to reach the calculated minimum and maximum loads stabilized, they were taken as the minimum and maximum deflections used for testing under displacement control. The loading wave form was sinusoidal. The minimum and maximum displacements used for each specimen can be found in Appendix B. During the fatigue tests, the applied test loads required to reach the deflections were less then static loads due to the dynamic amplification from the mass of the loading box and specimens.

4.2 TESTING SPEED

The typical testing frequency for the testing of specimens was 1.75 Hz. This testing speed was chosen since it was the maximum speed at which rubbing of the hydraulic hoses was not severe. Quicker testing speeds were possible, however due to the short fatigue lives of the specimens faster cyclic loading rates were not required.

4.3 DEFINITION OF FAILURE

Failure of a high-mast lighting tower specimen was defined as a 10% overall reduction in the loads required to attain the minimum and maximum displacements under displacement-control of the hydraulic actuator. The 10% load reduction was set as an interlock limit in the MTS controller. Once the interlock limit was triggered, the controller would stop the test.

CHAPTER 5

Test Results

5.1 FATIGUE TEST RESULTS

The results of fatigue testing of the high-mast lighting pole specimens are presented in the following sections of this chapter. Similar to the order in Chapter 2, the results for each connection type will be discussed beginning with the fillet welded socket connection, then continuing with the full penetration welded connections and finally the stool base connection detail. Following the discussion of each connection type individually, a general comparison of fatigue life for all connection types will be made.

5.1.1 Results for Fillet Welded Socket Connections

A total of 10 specimens utilizing the fillet welded socket connections were tested. Both 8-bolt and 12-bolt hole patterns were tested with the fillet welded socket connection detail. In addition, the base plate thickness was varied from 1½-in to 3-in.

The typical failure of the fillet welded socket connection detail was a crack through the wall of the pole, which followed the toe of the socket weld. This crack initiated at the top of the specimen, the extreme tension fiber. Typically, when a specimen was declared failed, the crack had extended to an approximate length of 15-in to 20-in. along the weld toe. Pictures of a typical failure can be found in Figure 5.1. The extent of cracking is shown by the black marker lines.

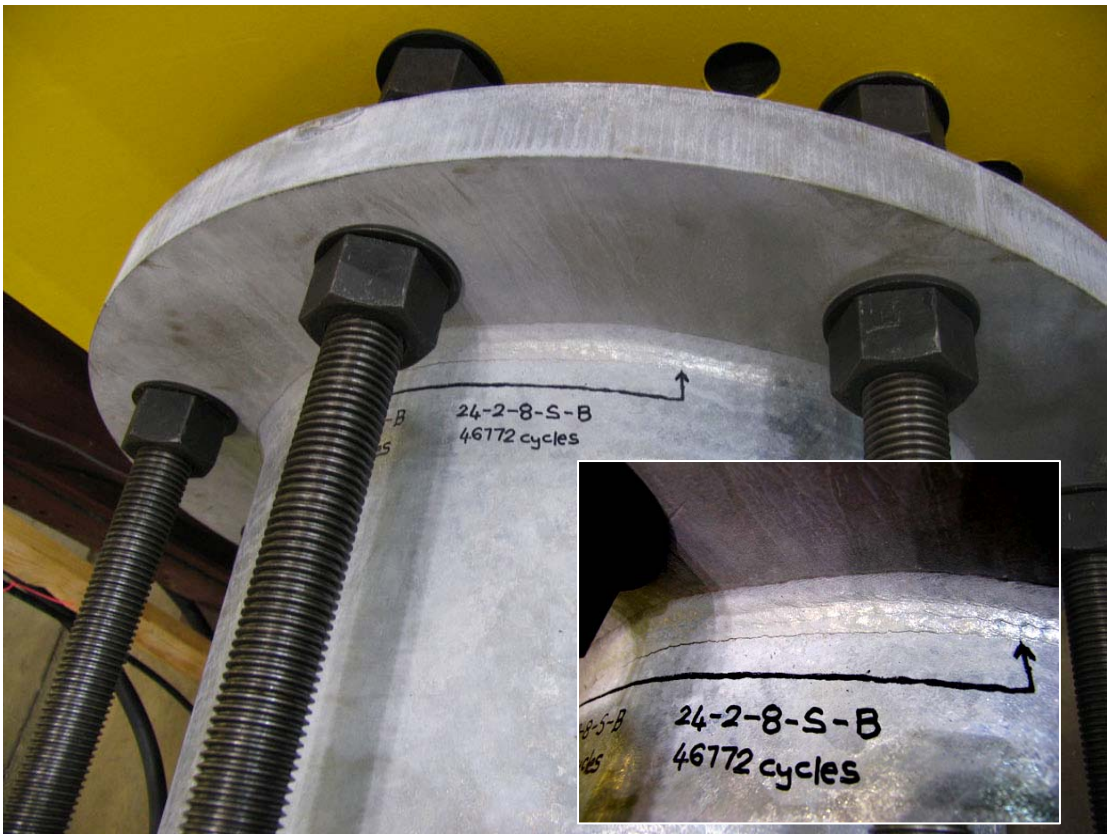

Figure 5.1: Typical failure of fillet welded socket connection

After testing, a cross section of a fillet welded socket connection specimen was cut with an acetylene torch, then ground, polished, and etched with a nitric acid solution. The etching reveals the weld and the amount of weld penetration. The etched cross section can be seen in Figure 5.2. The fracture initiated at the toe of the weld and then propagated through the pole wall. The unequal leg weld profile is also shown in the figure. The etching revealed that the weld was done in two passes.

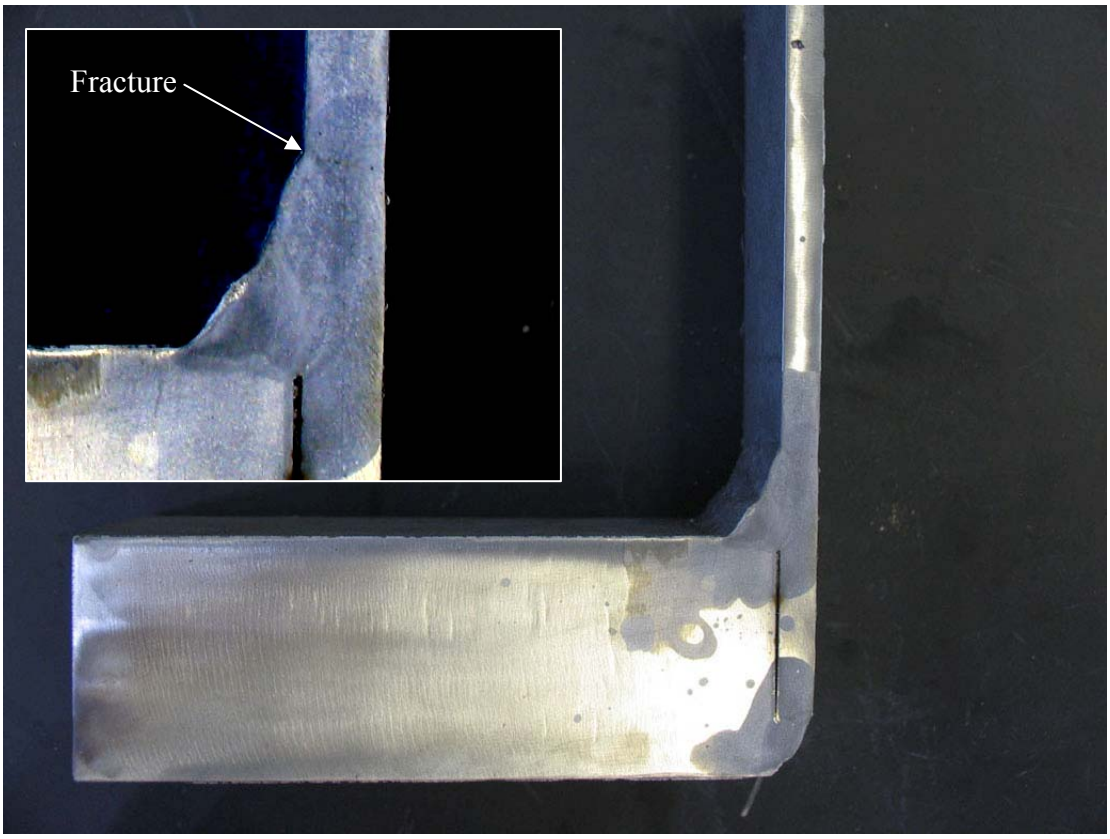

Figure 5.2: Etched cross section of fillet welded socket connection

The results of fatigue testing on the fillet welded socket connection specimens are summarized in Table 5.1. Specimens that utilized a 12-bolt hole pattern are shown in red font. Note that the number of bolt holes used in the base plates had an effect on the fatigue life of the pole. Increasing the number of bolt holes from 8 to 12 doubled the fatigue life in the 1.5-in base plate and almost tripled the life of the specimens with 2-in base plates. The 2-in base plate with 12 bolt holes had about the same performance as a 3-in base plate with 8 bolt holes.

The data also shows the effect that base plate thickness has on fatigue life. For the 8-bolt hole pattern, fatigue life increased by about 3.5 times when the base plate thickness was increased from 1.5-in to 2-in and increased by about 10 times when it was increased from a 1.5-in to a 3-in base plate.

Table 5.1: Fatigue testing results for fillet welded socket connection specimens

Specimen(s)	# Bolts	Base Plate Thickness (in)	Failure (10% drop in load)
24-1.5-8-S-A,B	8	1.5	13,193
24-1.5-12-S-A,B	12	1.5	27,977
24-2-8-S-A,B	8	2	46,772
24-2-12-S-A,B	12	2	143,214
24-3-8-S-A,B	8	3	147,550

(Replicate specimens had same fatigue life)

5.1.2 Results for Full Penetration Weld Connections

A total of 4 specimens using a full penetration weld connection were tested. Specimens using the Wyoming detail which utilized a back-up bar had an 8-bolt hole pattern with a 2-in base plate, and the specimens using the Texas detail had a 12-bolt hole pattern with a 3-in base plate.

The typical failure for both full penetration weld connection details was a crack through the wall of the pole, which followed the toe of the full penetration weld. Similar to the socketed connections, the crack initiated at the top of the specimen, the extreme tension fiber, and propagated approximately 15-in to 20-in before the specimen was declared failed. Pictures of typical failures for the Wyoming and Texas full penetration weld details can be found in Figure 5.3 and Figure 5.4, respectively.

Figure 5.3: Typical failure of Wyoming full penetration weld connection

Figure 5.4: Typical Failure of Texas full penetration weld connection

After testing was completed on the full penetration weld connection specimens, cross sections from both the Wyoming and Texas details were cut with an acetylene torch, then ground, polished, and etched with a nitric acid solution. The etched cross sections of the Wyoming and Texas details can be seen in Figure 5.5 and Figure 5.6, respectively. The fractures initiated at the weld toe, and then propagated through the pole wall.

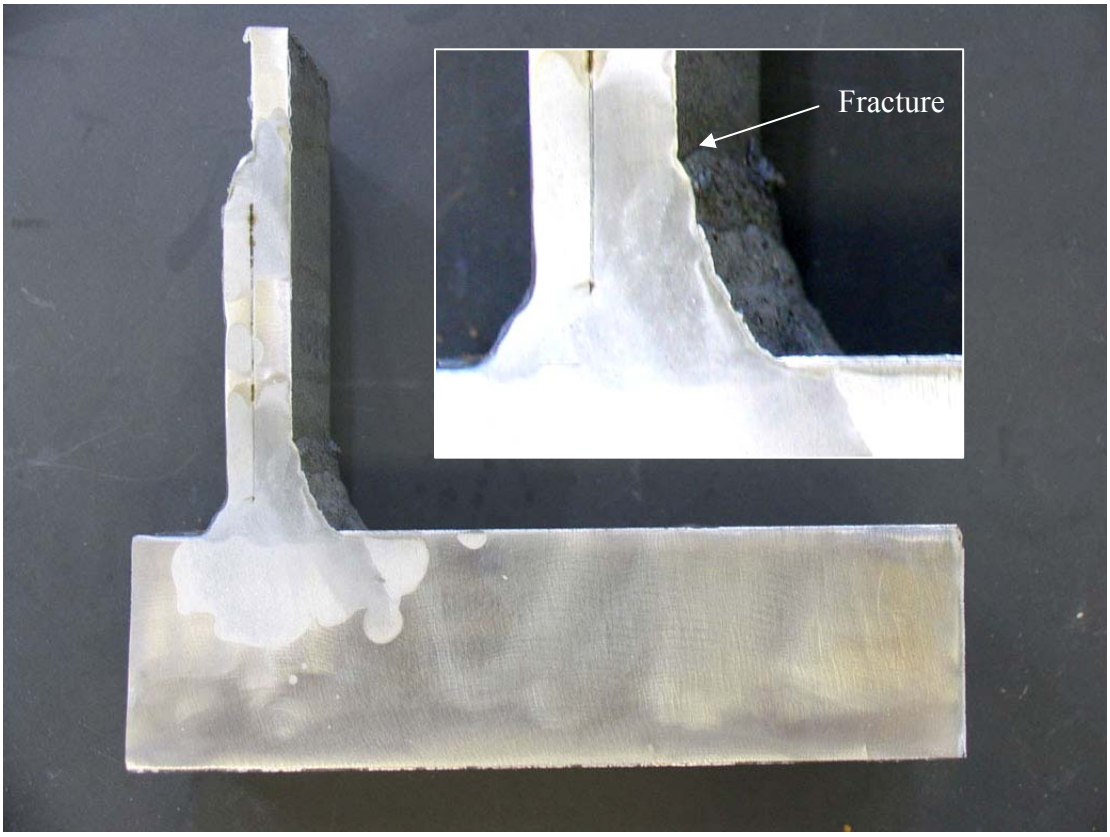

Figure 5.5: Etched cross section of Wyoming full penetration weld connection

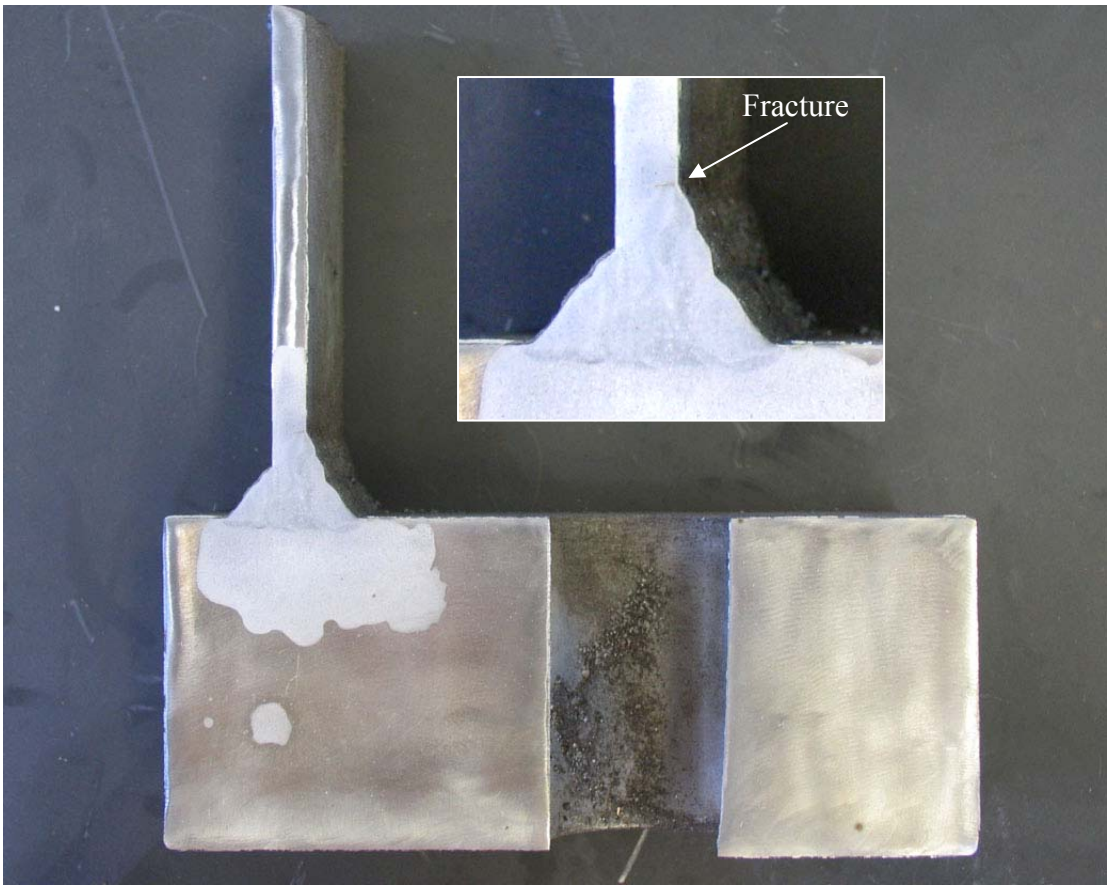

Figure 5.6: Etched cross section of Texas full penetration weld connection

The results of fatigue testing for the full penetration weld connections are summarized in Table 5.2. Both variations of the full penetration weld connections showed a noticeable improvement in fatigue resistance over the socketed connection. The Texas detail was able to reach around 2 or 2.5 times the number of cycles that the Wyoming detail was able to reach. However, it would not be just to directly compare the two types of full penetration weld details since the Wyoming detail has an 8-bolt hole pattern with a 2-in base plate and the Texas detail has a 12-bolt hole pattern with a 3-in base plate. It was seen in the results of the socketed connection that base plate thickness and number of bolt holes used has a noticeable effect on fatigue resistance.

Table 5.2: Fatigue testing results for full penetration weld connection specimens

Specimen(s)	# Bolts	Detail	Base Plate Thickness (in)	Failure (10% drop in load)
24-2-8-WY-A,B	8	Wyoming	2	133819*
24-3-12-TX-A,B	12	Texas	3	236,154 327,487

(* replicate specimens had same fatigue life)

5.1.3 Results for Stool Base Detail Connections

A total of 2 specimens using a stool base detail connection were tested. The stool base detail utilized an 8-bolt hole pattern in conjunction with a 2-in base plate.

The typical failure of the stool base connection detail was a crack through the wall of the pole. However, rather than failing the fillet weld at the base plate, fracture was initiated at the toe of the cap plate weld and then propagated following the weld toe and then into the pole wall. This is perhaps due to the transfer of load from the pole into the stiffeners. Pictures of a typical failure can be found in Figure 5.7.

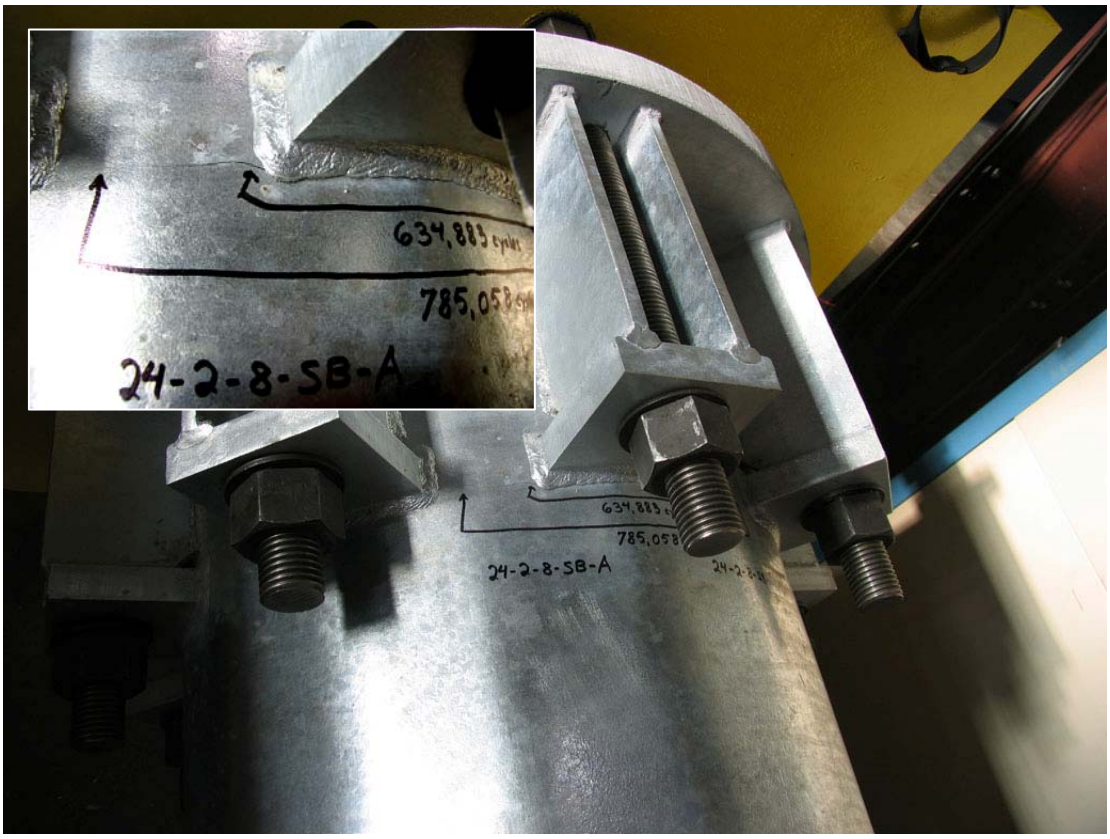

Figure 5.7: Typical failure of stool base detail connection

The results of fatigue testing for the stool base connection detail can be found in Table 5.3. The fatigue resistance of the stool base connection detail exceeded any other connection type. One specimen was able to reach almost 800,000 cycles.

Table 5.3: Fatigue testing results for stool base connection detail specimens

Specimen(s)	# Bolts	Base Plate Thickness (in)	Failure (10% drop in load)
24-2-8-SB-A,B	8	2	785,058 483,314

5.1.4 General comparison of fatigue life for all connection types

To compare the performance of all details, the fatigue lives of all specimens were plotted with the AASHTO fatigue design categories. The fatigue results can be seen on the S-N plot in Figure 5.8. Note that the only details to exceed Category E' were the stool base and Texas full penetration weld details. However, since the Texas detail uses a full penetration weld, the AASHTO design specification requires that it exceed Category E performance.

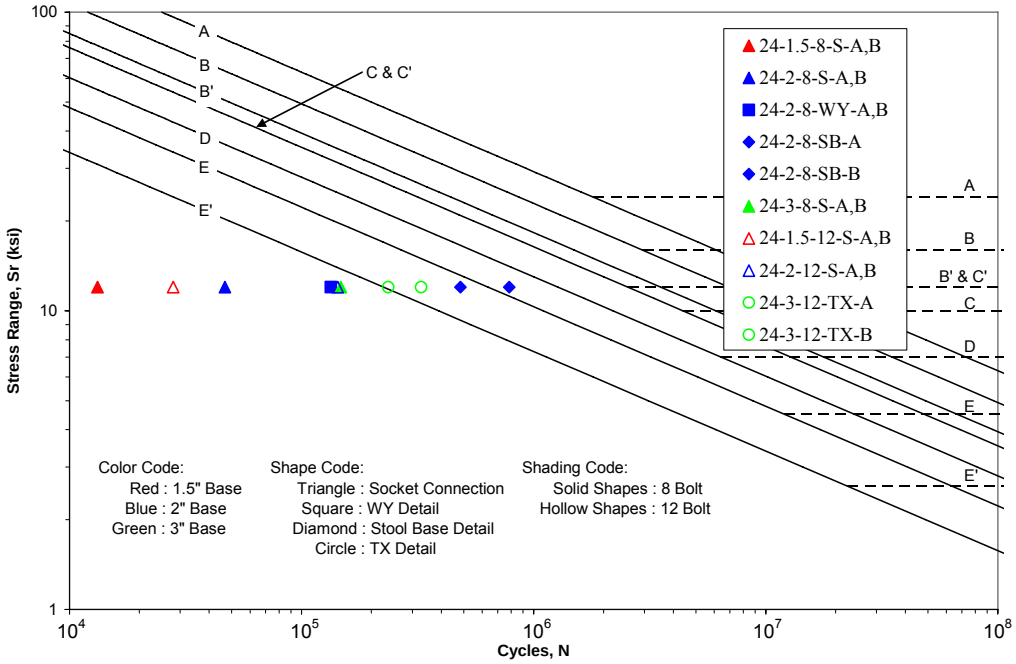

Figure 5.8: S-N plot of fatigue test results for all connection types

The plot also shows the effect of base plate thickness. One can see that the 1.5-in base plates (red symbols) performed the poorest, the 2-in base plates (blue) performed better than the 1.5-in base plates, and the 3-in base plates (green) performed the best.

The effect of number of bolt holes used in the base plates is also shown for both the 1½-in and 2-in plate thicknesses. For the socketed connection using a 1.5-in base plate, the 12-bolt exceeded the fatigue life of the 8-bolt in fatigue performance. The 2-in base plate socketed connection with a 12-bolt connection exceeded the 8-bolt fatigue life.

5.2 RESULTS OF TENSILE TESTS AND CHEMISTRY ANALYSIS

5.2.1 Tensile Test Results

In order to confirm the yield strength of the steel used in the high-mast lighting tower specimens, tensile tests were performed on three coupons obtained from the pole walls of the high-mast specimens. The tensile coupons were manufactured in accordance with ASTM A370. The test region was machined down to a width of 0.50-in with a 2-in gage length. The steel coupons were tested under displacement control. During testing, once the yield plateau was reached the displacement was stopped twice to obtain the static yield strength. A plot showing the stress vs. strain curves is shown in Figure 5.9.

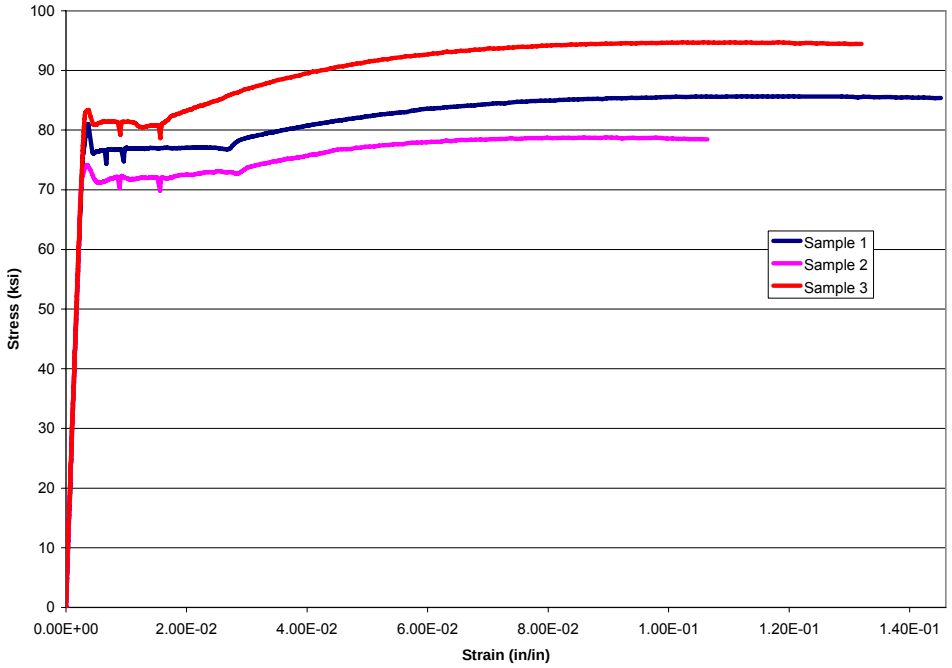

Figure 5.9: Tensile test results for pole wall steel coupons

The results of the three tensile tests are shown in Table 5.4. Along with the strength obtained from laboratory testing, the table also shows the mill test reported strengths. Comparing the measured values to the minimum specified values, two of the samples fulfilled the minimum requirements. However, one tensile test specimen did not meet the

required minimum ultimate strength. Specimen 2 showed an ultimate strength of 78.74-ksi which is 1.26-ksi short of the required minimum.

Table 5.4: Tensile test results

Specimen	Mill Test Strength		Laboratory Measured Strengths	
	Yield Strength (ksi)	Ultimate Strength (ksi)	Yield Strength (ksi)	Ultimate Strength (ksi)
1	77	95.9	74.95	85.67
2			70.05	78.74
3			78.92	94.69
Specified Minimum Values ASTM A572 Gr. 65	65	80		

5.2.2 Chemistry Analysis Results

Three samples were taken from the tensile testing coupons, and a chemical analysis was performed by Chicago Spectro Service Laboratory, Inc. in Chicago, IL. Tests for carbon and sulfur were performed in accordance with ASTM E1019, and tests for other elements were performed in accordance with ASTM E415. The results of the analyses are presented in Table 5.5. The maximum allowable limits for the specified elements are included in Table 5.5.

Table 5.5: Results of Chemistry Analysis

Elements	Specified Maximum Limit %	Specimens Tested		
		1	2	3
C	0.23	0.04	0.09	0.15
Mn	1.65	1.43	1.41	1.38
P	0.04	0.016	0.018	0.018
S	0.05	0.012	0.02	0.018
Si	0.40	0.04	0.02	0.04
Ni		0.07	0.02	0.08
Cr		0.04	0.01	0.13
Mo		0.03	0.04	0.03
Cu		0.36	0.06	0.28
Al		0.037	0.041	0.032
V		0.093	0.044	0.085
Ti		0.007	0.009	0.009
N		0.049	0.03	0.04

The specified grade steel for the test specimens was ASTM A572 Gr. A. The results of the chemistry analysis show that the steel met all of the requirements of ASTM A572 Gr. A.

CHAPTER 6

Conclusions and Recommended Research

6.1 CONCLUSIONS

The following conclusions can be made from this experimental research study:

- The research shows that the design provisions for high-mast lighting towers do not accurately predict the fatigue life of the structures. Common details designed in accordance with the AASHTO specification did not meet the required minimum fatigue life categories as specified by the design provisions. The fillet welded socket connections did not meet the Category E' requirements and the full penetration weld connections did not meet Category E requirements.
- A significant improvement in the fatigue life was found with an increase in base plate thickness. This improvement is not represented in the current AASHTO specification. Base plate thickness is not addressed in the fatigue design provisions.
- Increasing the number of bolts used in the base plates produced an increase in fatigue life. Much like base plate thickness, this improvement due to bolt geometry and number is not included in the current AASHTO specification. The bolted connection geometry and number of bolts is not addressed in the fatigue design provisions.
- The full penetration weld connections showed an improved fatigue resistance over the fillet welded socket connection. The full penetration weld connection using the Texas detail with a 3-in base plate and a 12 bolt connection was able to achieve a Category E' fatigue life. However, the AASHTO design specification requires a minimum fatigue life of Category E for full penetration weld connections.

- The stool base detail produced the best fatigue performance. Its fatigue performance was better then Category E' and just below Category E.
- Based upon the poor performance of the socket weld and full penetration weld specimens with base plates less than 3-in, it is recommended that 24-in diameter high-mast lighting towers should be designed with base plates 3-in or greater in thickness.

6.2 RECOMMENDED RESEARCH

Based on the test results found in this research and the previously stated conclusions, the following research is recommended:

- It is recommended that a parametric finite element analysis be performed on the connection details tested in this research. A parametric finite element analysis could be used to both verify the results found in this research as well as determine the effect of variables not investigated such as pole diameter or pole wall thickness.
- Test variables used in this research included connection type, base plate thickness, and the number of bolt holes used. Further laboratory fatigue testing should be conducted to investigate the effect of pole diameter as well as pole wall thickness.
- Previous research indicated that base plate flexibility has a significant effect on fatigue performance (Warpinksi, 2006). The test results in this study confirmed this when an improved fatigue performance was observed with thicker base plates. In full penetration weld connections, stiffer base plates can also be achieved by decreasing the inner diameter of the base plate. Laboratory fatigue testing should be performed to determine the effectiveness of decreasing the inner diameter of base plates used in full penetration weld connections.
- In light of current research being conducted at the University of Texas, base plate to pole connections utilizing an external collar show a significant improvement in fatigue life over fillet welded socket connections as well as full penetration weld

connections. It is recommended that laboratory fatigue testing be performed on high-mast pole specimens that utilize an external collar.

- Due to the good performance of the stool base connection detail, further laboratory fatigue testing should be performed on this detail. However, in lieu of using individual cap plates at the ends of the vertical stiffeners, a continuous ring should be used in the design of the connection. A continuous ring would distribute stresses more evenly in the pole wall than would individual cap plates. This would perhaps reduce the stress concentrations leading to improved fatigue life.

APPENDIX A

Measured Dimensions of Test Specimens

Table A1: General Dimensions- Diameters at base to flats

Specimen	Diameter at Base to Flats (in)			
	1	2	Average	Out of Round %
24-1.5-8-S-A	23.375	23.375	23.375	0.000
24-1.5-8-S-B	23.375	23.375	23.375	0.000
24-2-8-S-A	23.344	23.344	23.344	0.000
24-2-8-S-B	23.375	23.344	23.359	0.134
24-2-8-WY-A	23.125	23.375	23.250	1.070
24-2-8-WY-B	23.563	23.188	23.375	1.592
24-3-8-S-A	23.469	23.375	23.422	0.399
24-3-8-S-B	23.375	23.344	23.359	0.134
24-2-8-SB-A	23.344	23.344	23.344	0.000
24-2-8-SB-B	23.313	23.344	23.328	0.134
24-1.5-12-S-A	23.313	23.375	23.344	0.267
24-1.5-12-S-B	23.281	23.344	23.313	0.268
24-2-12-S-A	23.375	23.313	23.344	0.267
24-2-12-S-B	23.344	23.313	23.328	0.134
24-3-12-TX-A	23.344	23.406	23.375	0.267
24-3-12-TX-B	23.563	23.563	23.563	0.000

Table A2: General Dimensions- Diameter at base to corners

Specimen	Diameter at Base to Corners (in)			
	1	2	Average	Out of Round %
24-1.5-8-S-A	23.594	23.625	23.609	0.132
24-1.5-8-S-B	23.625	23.625	23.625	0.000
24-2-8-S-A	23.563	23.563	23.563	0.000
24-2-8-S-B	23.625	23.594	23.609	0.132
24-2-8-WY-A	23.500	23.594	23.547	0.397
24-2-8-WY-B	23.688	23.438	23.563	1.055
24-3-8-S-A	23.563	23.594	23.578	0.132
24-3-8-S-B	23.625	23.594	23.609	0.132
24-2-8-SB-A	23.563	23.563	23.563	0.000
24-2-8-SB-B	23.531	23.594	23.563	0.265
24-1.5-12-S-A	23.594	23.625	23.609	0.132
24-1.5-12-S-B	23.531	23.656	23.594	0.528
24-2-12-S-A	23.594	23.563	23.578	0.132
24-2-12-S-B	23.563	23.563	23.563	0.000
24-3-12-TX-A	23.594	23.656	23.625	0.264
24-3-12-TX-B	23.813	23.813	23.813	0.000

Table A3: General Dimensions- Diameter 12-in away from base to flats

Specimen	Diameter at 12" to Flats (in)			
	1	2	Average	Pole Taper (in/ft)
24-1.5-8-S-A	23.156	23.250	23.203	0.172
24-1.5-8-S-B	23.188	23.250	23.219	0.156
24-2-8-S-A	23.156	23.188	23.172	0.172
24-2-8-S-B	23.250	23.219	23.234	0.125
24-2-8-WY-A	22.906	23.313	23.109	0.141
24-2-8-WY-B	23.313	23.063	23.188	0.188
24-3-8-S-A	23.188	23.188	23.188	0.234
24-3-8-S-B	23.219	23.219	23.219	0.141
24-2-8-SB-A	23.281	23.219	23.250	0.094
24-2-8-SB-B	23.156	23.250	23.203	0.125
24-1.5-12-S-A	23.156	23.281	23.219	0.125
24-1.5-12-S-B	23.156	23.281	23.219	0.094
24-2-12-S-A	23.219	23.188	23.203	0.141
24-2-12-S-B	23.156	23.156	23.156	0.172
24-3-12-TX-A	23.250	23.250	23.250	0.125
24-3-12-TX-B	23.375	23.375	23.375	0.188

Table A4: General Dimensions- Diameter 12-in away from base to corners

Specimen	Diameter at 12" to Corners (in)			
	1	2	Average	Pole Taper (in/ft)
24-1.5-8-S-A	23.406	23.200	23.303	0.306
24-1.5-8-S-B	23.438	23.500	23.469	0.156
24-2-8-S-A	23.500	23.406	23.453	0.110
24-2-8-S-B	23.500	23.438	23.469	0.141
24-2-8-WY-A	23.281	23.531	23.406	0.141
24-2-8-WY-B	23.625	23.313	23.469	0.094
24-3-8-S-A	23.438	23.406	23.422	0.156
24-3-8-S-B	23.469	23.406	23.438	0.172
24-2-8-SB-A	23.438	23.500	23.469	0.094
24-2-8-SB-B	23.406	23.531	23.469	0.094
24-1.5-12-S-A	23.406	23.500	23.453	0.156
24-1.5-12-S-B	23.375	23.531	23.453	0.141
24-2-12-S-A	23.438	23.438	23.438	0.141
24-2-12-S-B	23.438	23.469	23.453	0.109
24-3-12-TX-A	23.500	23.500	23.500	0.125
24-3-12-TX-B	23.656	23.625	23.641	0.172

Table A5: General Dimensions- Base plate thickness

Specimen	Base Plate Thickness (in)					
	1	2	3	Average	Specified	% Difference
24-1.5-8-S-A	1.531	1.528	1.529	1.529	1.5	1.956
24-1.5-8-S-B	1.537	1.528	1.531	1.532	1.5	2.133
24-2-8-S-A	2.090	2.092	2.082	2.088	2	4.400
24-2-8-S-B	2.070	2.075	2.055	2.067	2	3.333
24-2-8-WY-A	2.094	2.092	2.093	2.093	2	4.650
24-2-8-WY-B	2.092	2.091	2.090	2.091	2	4.550
24-3-8-S-A	3.052	3.048	3.055	3.052	3	1.722
24-3-8-S-B	3.042	3.048	3.065	3.052	3	1.722
24-2-8-SB-A	2.096	2.073	2.091	2.087	2	4.333
24-2-8-SB-B	2.085	2.080	2.092	2.086	2	4.283
24-1.5-12-S-A	1.527	1.531	1.525	1.528	1.5	1.844
24-1.5-12-S-B	1.533	1.531	1.531	1.532	1.5	2.111
24-2-12-S-A	2.050	2.050	2.059	2.053	2	2.650
24-2-12-S-B	2.069	2.066	2.060	2.065	2	3.250
24-3-12-TX-A	3.037	3.037	3.043	3.039	3	1.300
24-3-12-TX-B	3.050	3.050	3.033	3.044	3	1.478

Table A6: General Dimensions- Pole wall thickness

Specimen	Pole Wall Thickness (in)					
	1	2	3	Average	Specified	% Difference
24-1.5-8-S-A	0.340	0.332	0.329	0.334	0.3125	6.773
24-1.5-8-S-B	0.330	0.333	0.328	0.330	0.3125	5.707
24-2-8-S-A	0.339	0.337	0.331	0.336	0.3125	7.413
24-2-8-S-B	0.341	0.335	0.335	0.337	0.3125	7.840
24-2-8-WY-A	0.342	0.343	0.341	0.342	0.3125	9.440
24-2-8-WY-B	0.337	0.338	0.335	0.337	0.3125	7.733
24-3-8-S-A	0.334	0.333	0.334	0.334	0.3125	6.773
24-3-8-S-B	0.337	0.333	0.331	0.334	0.3125	6.773
24-2-8-SB-A	0.336	0.332	0.333	0.334	0.3125	6.773
24-2-8-SB-B	0.335	0.332	0.329	0.332	0.3125	6.240
24-1.5-12-S-A	0.333	0.339	0.334	0.335	0.3125	7.307
24-1.5-12-S-B	0.338	0.336	0.331	0.335	0.3125	7.200
24-2-12-S-A	0.329	0.332	0.329	0.330	0.3125	5.600
24-2-12-S-B	0.343	0.337	0.334	0.338	0.3125	8.160
24-3-12-TX-A	0.327	0.329	0.329	0.328	0.3125	5.067
24-3-12-TX-B	0.330	0.333	0.331	0.331	0.3125	6.027

Table A7: Socket Weld Dimensions- Long leg dimensions

Specimen	Long Leg On Pole Wall (in)					
	1	2	3	Average	Specified	% Difference
24-1.5-8-S-A	0.813	0.813	0.750	0.792	0.62	27.688
24-1.5-8-S-B	0.719	0.750	0.719	0.729	0.62	17.634
24-2-8-S-A	0.688	0.719	0.719	0.708	0.62	14.247
24-2-8-S-B	0.719	0.688	0.688	0.698	0.62	12.567
24-3-8-S-A	0.688	0.688	0.688	0.688	0.62	10.887
24-3-8-S-B	0.688	0.750	0.750	0.729	0.62	17.608
24-2-8-SB-A	0.656	0.719	0.656	0.677	0.62	9.207
24-2-8-SB-B	0.813	0.813	0.875	0.833	0.62	34.409
24-1.5-12-S-A	0.813	0.750	0.813	0.792	0.62	27.688
24-1.5-12-S-B	0.688	0.688	0.750	0.708	0.62	14.247
24-2-12-S-A	0.750	0.750	0.750	0.750	0.62	20.968
24-2-12-S-B	0.813	0.813	0.875	0.833	0.62	34.409

Table A8: Socket Weld Dimensions- Short leg dimensions

Specimen	Short Leg on Base Plate (in)					
	1	2	3	Average	Specified	% Difference
24-1.5-8-S-A	0.438	0.375	0.375	0.396	0.37	6.982
24-1.5-8-S-B	0.438	0.375	0.406	0.406	0.37	9.820
24-2-8-S-A	0.469	0.406	0.406	0.427	0.37	15.428
24-2-8-S-B	0.344	0.438	0.375	0.385	0.37	4.167
24-3-8-S-A	0.438	0.469	0.406	0.438	0.37	18.243
24-3-8-S-B	0.438	0.469	0.469	0.458	0.37	23.874
24-2-8-SB-A	0.438	0.344	0.375	0.385	0.37	4.167
24-2-8-SB-B	0.406	0.406	0.875	0.563	0.37	52.027
24-1.5-12-S-A	0.406	0.438	0.406	0.417	0.37	12.613
24-1.5-12-S-B	0.469	0.438	0.469	0.458	0.37	23.874
24-2-12-S-A	0.438	0.469	0.438	0.448	0.37	21.059
24-2-12-S-B	0.438	0.375	0.375	0.396	0.37	6.982

Table A9: Full Penetration Weld Dimensions- Long leg dimensions

Specimen	Long Leg On Pole Wall (in)					
	1	2	3	Average	Specified	% Difference
24-2-8-WY-A	0.875	0.813	0.813	0.834	0.75	11.156
24-2-8-WY-B	0.813	0.813	0.813	0.813	0.75	8.333
24-3-12-TX-A	0.750	0.750	0.750	0.750	0.62	20.968
24-3-12-TX-B	0.750	0.750	0.750	0.750	0.62	20.968

Table A10: Full Penetration Weld Dimensions- Short leg dimensions

Specimen	Short Leg on Base Plate (in)					
	1	2	3	Average	Specified	% Difference
24-2-8-WY-A	0.406	0.438	0.344	0.396	0.31	27.742
24-2-8-WY-B	0.375	0.344	0.344	0.354	0.31	14.247
24-3-12-TX-A	0.438	0.531	0.469	0.479	0.37	29.505
24-3-12-TX-B	0.438	0.438	0.500	0.458	0.37	23.874

Table A11: Stool Base Detail Dimensions- Stiffener dimensions

Specimen	Stiffener	Dimension A	Dimension B	Dimension C	Dimension D
24-2-8-SB-A	1	10.969	1.260	2.985	0.508
	2	10.969	1.260	2.973	0.513
	3	10.938	1.257	2.952	0.511
	Average	10.958	1.259	2.970	0.511
24-2-8-SB-B	1	11.000	1.262	2.990	0.509
	2	10.938	1.261	2.939	0.512
	3	10.969	1.265	3.000	0.509
	Average	10.969	1.263	2.976	0.510

*See Figure A.1 for locations of stiffener dimensions

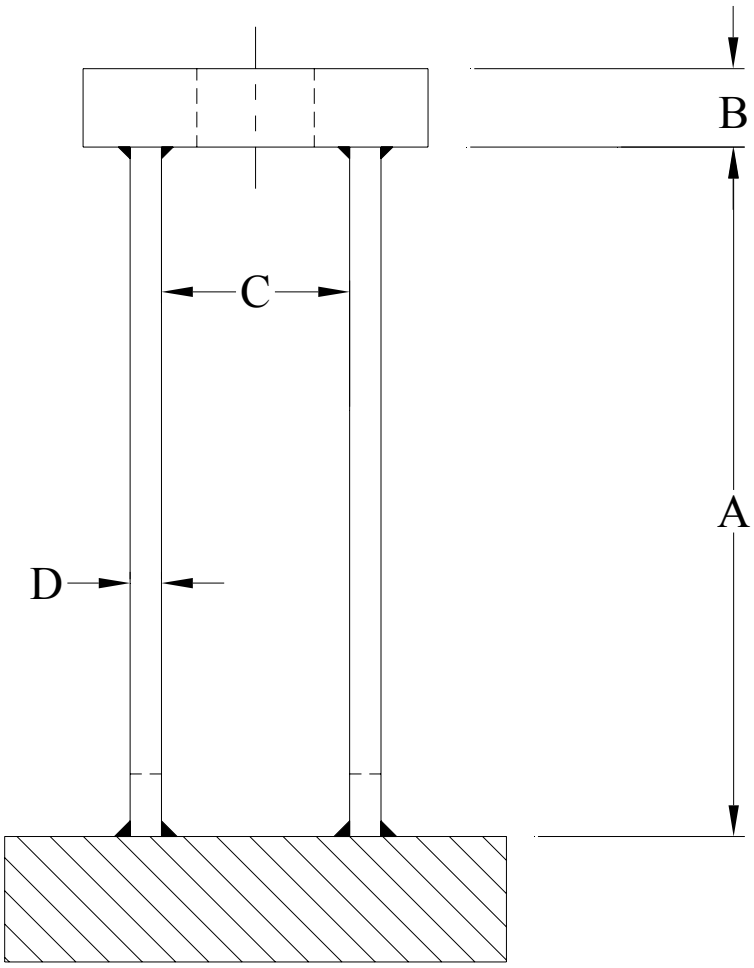

Figure A1: Locations of dimensions for stool base stiffeners

APPENDIX B

Calculated Loads and Displacements for Fatigue Testing

Table B1: Calculate properties from AutoCAD using average dimensions

Specimen	Moment of Inertia (in^4)	Distance to Extreme Fiber, C (in)
24-1.5-8-S-A,B	1691.35	12
24-2-8-S-A,B	1791.394	12.156
24-2-8-WY-A,B	1804.482	12.145
24-3-8-S-A,B	1788.901	12.175
24-2-8-SB-A,B	1771.148	12.151
24-1.5-12-S-A,B	1787.675	12.161
24-2-12-S-A,B	1776.693	12.152
24-3-12-TX-A,B	1784.095	12.216

Table B2: Calculated ram loads to achieve desired stresses

Specimen	P_{min} (kips)	P_{max} (kips)
24-1.5-8-S-A,B	15.827	34.82
24-2-8-S-A,B	16.593	36.505
24-2-8-WY-A,B	16.729	36.804
24-3-8-S-A,B	16.631	36.589
24-2-8-SB-A,B	16.412	36.106
24-1.5-12-S-A,B	16.5	36.299
24-2-12-S-A,B	16.462	36.216
24-3-12-TX-A,B	16.532	36.371

Table B3: Testing displacements and corresponding values

Specimen	Min Testing Displacement (in)	Max Testing Displacement (in)	Target Ram Setpoint (in)	Testing Amplitude (in)	Testing Frequency (Hz)
24-1.5-8-S-A,B	-2.305	-1.601	-1.953	0.352	0.8
24-2-8-S-A,B	-1.95	-1.331	-1.6405	0.3095	1.75
24-2-8-WY-A,B	-2.246	-1.669	-1.9575	0.2885	1.75
24-3-8-S-A,B	-2.219	-1.677	-1.948	0.271	1.75
24-2-8-SB-A,B	-2.462	-2.012	-2.237	0.225	2.25
24-1.5-12-S-A,B	-2.236	-1.608	-1.922	0.314	1.75
24-2-12-S-A,B	-2.163	-1.606	-1.8845	0.2785	1.75
24-3-12-TX-A,B	-2.168	-1.679	-1.9235	0.2445	1.75

REFERENCES

1. American Association of State Highway and Transportation Officials, AASHTO Standard Specifications for Structural Supports for Highway Signs, Luminaries and Traffic Signals. Fourth Edition, AASHTO, Washington, D.C., 2001.

2. FlexTest SE User Information and Software Reference, MTS Systems Corporation, 2004.

3. Kaczinski, M.R., et al., Fatigue-Resistant Design of Cantilevered Signals, Sign, and Light Supports. National Cooperative Highway Research Program, NCHRP Report 412, Transportation Research Board, Washington, D.C., 1998.

4. Koenigs, M.T.K., Fatigue Resistance of Traffic Signal Mast-Arm Connection Details. M.S. Thesis, Department of Civil Engineering, The University of Texas at Austin, May 2003.

5. Koenigs, et al., Fatigue Resistance of Traffic Signal Mast-Arm Connections. Texas Department of Transportation, Research Report 4178-2, Center for Transportation Research, August 2003.

6. Miki, Chitoshi, Fisher, J.W., Slutter, R.G., Fatigue Behavior of Steel Light Poles. Report No. 200.81.714.1. Fritz Engineering Laboratory, Lehigh University, 1984.

7. Ocel, J.M., The Behavior of Thin Hollow Structural Section (HSS) to Plate Connections. Dissertation, The Department of Civil Engineering, The University of Minnesota, October, 2006.

8. Simiu, E., Scanlan, R., Wind Effects on Structures: Fundamentals and Applications to Design. Third Edition, John Wiley & Sons, New York, 1996.

9. Sockel, H., Wind-Excited Vibrations of Structures. CISM Courses and Lectures NO. 335, International Centre for Mechanical Sciences, 1994.

10. Walton, N.E., Rowan, N.J., High-mast Lighting. Texas Transportation Institute, Report 75-12, Texas Highway Department, February 1969.

11. Walton, N.E., Rowan, N.J., Interim Progress Report on Supplementary Studies in Highway Illumination. Texas Transportation Institute, Report 75-7, Texas Highway Department, October 1967.

12. Warpinski, M.K., The Effect of Base Connection Geometry on the Fatigue Performance of Welded Socket Connections in Multi-sided High-mast Lighting Towers. M.S. Thesis, Department of Civil Engineering, Lehigh University, May 2006.

VITA

Craig Abel Rios was born in San Antonio, Texas on April 12, 1982, to Dinia Cantu Rios and Raul Almaguer Rios. After completing his work at Antonian College Preparatory High School, San Antonio, Texas in 2001, he enrolled at The University of Texas at Austin. He received a Bachelor of Science in Civil Engineering from The University of Texas at Austin in May of 2005. Craig enrolled in the graduate program at The University of Texas at Austin in August of 2005.

Permanent Address: 139 Cornwall
San Antonio, TX 78216
rios8033@gmail.com

This thesis was typed by the author.